Received: 24 November 2019 | Revised: 23 April 2020 | Accepted: 27 April 2020

DOI: 10.1111/bre.12462

ORIGINAL ARTICLE

Basin Research IAS EAGE WILEY

Sediment dispersal and redistributive processes in axial and transverse deep-time source-to-sink systems of marine rift basins: Dampier Sub-basin, Northwest Shelf, Australia

Hehe Chen[1,2,3] | **Lesli J. Wood**[1] | **Robert L. Gawthorpe**[2]

[1]Department of Geology and Geological Engineering, Colorado School of Mines, Golden, CO, USA

[2]Department of Earth Science, University of Bergen, Bergen, Norway

[3]College of Geosciences, China University of Petroleum, Beijing, China

Correspondence
Hehe Chen, Department of Geology and Geological Engineering, Colorado School of Mines, Golden, CO, USA.
Emails: hehechen89@gmail.com, chenhe_cup@163.com

Abstract

Morphological scaling relationships between source-to-sink segments have been widely explored in modern settings, however, deep-time systems remain difficult to assess due to limited preservation of drainage basins and difficulty in quantifying complex processes that impact sediment dispersals. Integration of core, well-logs and 3-D seismic data across the Dampier Sub-basin, Northwest Shelf of Australia, enables a complete deep-time source-to-sink study from the footwall (Rankin Platform) catchment to the hanging wall (Kendrew Trough) depositional systems in a Jurassic late syn-rift succession. Hydrological analysis identifies 24 drainage basins on the J50.0 (Tithonian) erosional surface, which are delimited into six drainage domains confined by NNE-SSW trending grabens and their horsts, with drainage domain areas ranging between 29 and 156 km^2. Drainage outlets of these drainage domains are well preserved along the Rankin Fault System scarp, with cross-sectional areas ranging from 0.08 to 0.31 km^2. Corresponding to the six drainage domains, sedimentological and geomorphological analysis identifies six transverse submarine fan complexes developing in the Kendrew Trough, ranging in areas from 43 to 193 km^2. Seismic geomorphological analysis reveals over 90-km-long, slightly sinuous axial turbidity channels, developing in the lower topography of the Kendrew Trough which erodes toe parts of transverse submarine fan complexes. Positive scaling relationships exist between drainage outlet spacing and drainage basin length, and drainage outlet cross-sectional area and drainage basin area, which indicates the geometry of drainage outlets can provide important constraints on source area dimensions in deep-time source-to-sink studies. The broadly negative bias of fan area to drainage basin area ratios indicates net sediment losses in submarine fan complexes caused by axial turbidity current erosion. Source-to-sink sediment balance studies must be done with full evaluating of adjacent source-to-sink systems to delineate fans and their associated up-dip drainages, to achieve an accurate tectonic and sedimentologic picture of deep-time basins.

KEYWORDS
drainage basin, rift, seismic geomorphology, source-to-sink, submarine fan, turbidity current

1 | INTRODUCTION

Source-to-sink (S2S) studies examine the long-term variations in sediment flux in coupled erosional and depositional systems and the corresponding morphologic evolution of these systems (e.g., Anderson, Wallace, Simms, Rodriguez, & Taha, 2016; Bhattacharya, Copeland, Lawton, & Holbrook, 2016; Helland-Hansen, Sømme, Martinsen, Lunt, & Thurmond, 2016; Sømme, Helland-Hansen, Martinsen, & Thurmond, 2009). Deep-time S2S studies generally involve the reconstruction of drainage basins, the sediment-routing systems and the features of depositional systems in the sink (e.g., Bhattacharya et al., 2016; Helland-Hansen et al., 2016; Sømme, Jackson, & Vaksdal, 2013). Focusing on modern and sub-modern S2S systems, some authors have suggested a variety of morphological scaling relationships that may exist between a drainage basin (e.g., width and length) and the basin's submarine fan (e.g., Nyberg et al., 2018; Sømme et al., 2009; Sømme & Jackson, 2013; Sømme, Jackson, et al., 2013). Whereas in ancient S2S systems, drainage basins are often only partly preserved at best, or, if relatively intact, are poorly imaged in the subsurface (e.g., Matenco & Andriessen, 2013; Sømme et al., 2009). Without drainage basin preservation, other morphological topographic parameters, such as drainage outlet morphology, may be utilized to achieve a first approximation of the nature and discharge of ancient S2S systems (e.g., Ethridge, Germanoski, Schumm, & Wood, 2005; Mattheus & Rodriguez, 2011; Mattheus, Rodriguez, Greene, Simms, & Anderson, 2007). However, the use of such relationships remains largely untested and the accuracy of such methods is unknown.

Rift basins have long been the topic of many S2S studies, in part driven by their narrow floodplains and shelves which results in the development of shorter, less buffered S2S systems (e.g., Sømme et al., 2009). Topics of such studies include the landscape evolution of individual footwall blocks (e.g., Densmore, Dawers, Gupta, Allen, & Gilpin, 2003; Densmore, Dawers, Gupta, & Guidon, 2005; Dibiase, Whipple, Heimsath, & Ouimet, 2010; Duffy, Brocklehurst, Gawthorpe, Leeder, & Finch, 2015), the influence of sediment budget on hanging wall depositional systems (e.g., Chen, Zhu, Wood, & Shi, 2019; Liu et al., 2019) and rifts as a whole (e.g., Pechlivanidou et al., 2019; Watkins et al., 2018). Although most of such S2S studies focus on the single catchment-fan system developed in the footwall or hanging wall of rift basins, such studies seldom incorporate the influences of axial sediment routing on these transverse depositional systems (e.g., Chen et al., 2019; Connell, Kim, Paola, & Smith, 2012; Gawthorpe & Leeder, 2000; Leeder, 2011). S2S rift basin is to be composed of structurally and hydrodynamically complex S2S segments, and these cannot be studied in isolation if we are to fully understand sediment dispersal in these basins (e.g., Helland-Hansen et al., 2016; Nyberg et al., 2018; Sømme & Jackson, 2013; Sømme, Jackson, et al., 2013).

Highlights

- The dimension of drainage outlets is positive to the drainage basin area, providing a good approximation of source dimensions.
- Axial turbiditic channels toe-cut transverse submarine fans, resulting in sediment redistribution between transverse S2S systems.
- Evaluating adjacent S2S systems together is critical to tie individual fans to their updip feeding drainage basins.

The complexity and scarcity of S2S rift basin system studies have led us to examine the relationship between drainage basin morphology and footwall-source transverse depositional systems, and the impact of axial sediment routing (i.e., parallel to structure) on basin fill. This study focuses on the Jurassic-to-Early Cretaceous rift interval in the Dampier Sub-basin of the Northwest Shelf of Australia (Figure 1). We utilize seismic geomorphological analysis, integrated with well-logs and core data, to evaluate the sediment dispersal and redistributive processes between transverse and axial S2S routing segments. The specific objectives of this study are to (1) restore the palaeo-morphology of the rift footwalls and quantify the footwall drainage catchments; (2) examine the sedimentology of footwall depositional systems and their morphological parameters (e.g., width, length and area) and (3) assess scaling relationships between S2S segments and examine the influences on the morphometrics and sediment budgets of ancient rift systems. The results of this study advance our understand of morphometric scaling relationships of rift basin elements, and inform our knowledge of sediment dispersal and redistribute processes in marine rift basins, new knowledge which enlightens other ancient S2S studies worldwide.

2 | GEOLOGICAL SETTING AND STRATIGRAPHY

The Dampier Sub-basin is a Jurassic-to-Early Cretaceous marine rift basin in the Northern Carnarvon Basin,

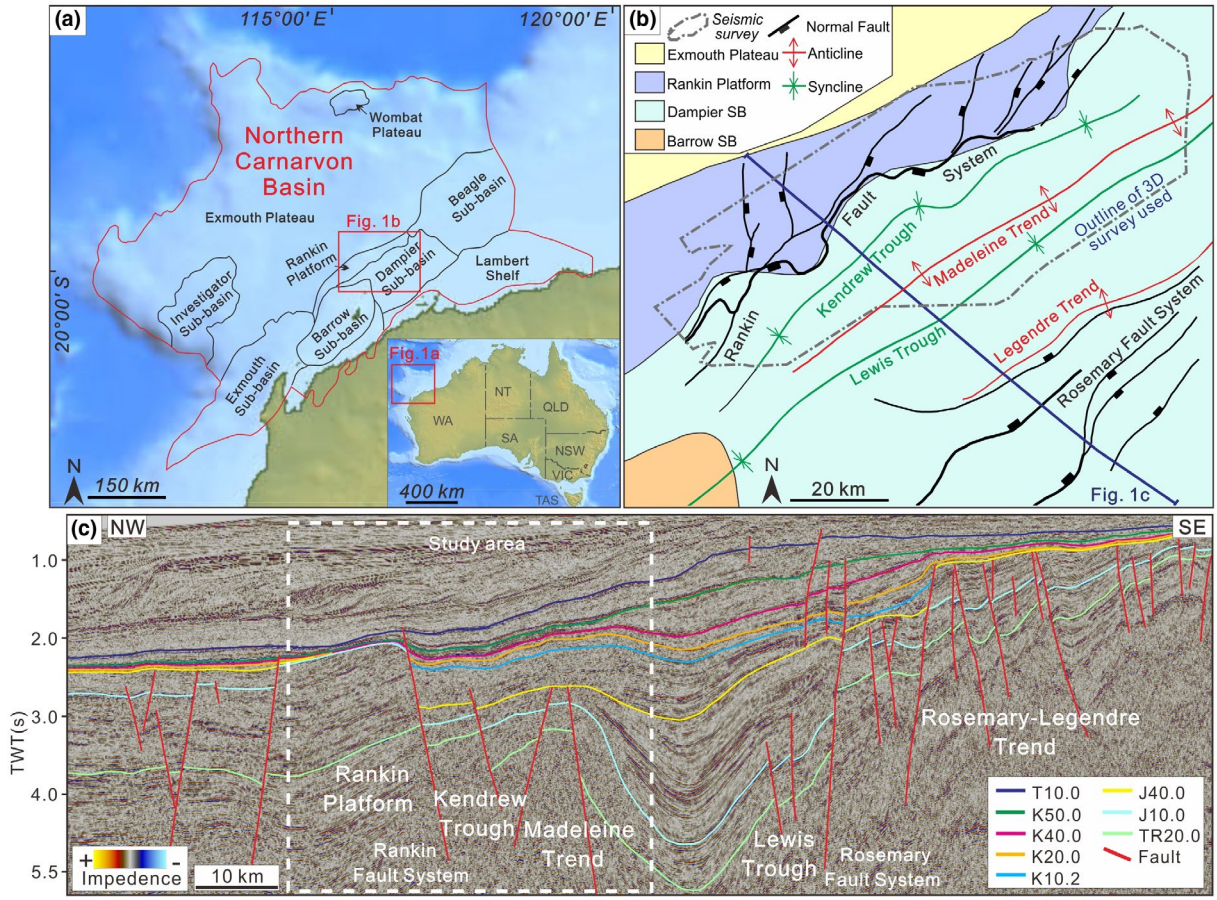

FIGURE 1 (a) Structural elements map of the Northern Carnarvon Basin showing the location of Dampier Sub-basin (after Stagg, 2004). (b) Map showing the main structural elements and faults in the Dampier Sub-basin with seismic survey used in the study highlighted (after Stagg, 2004). (c) Interpreted seismic sections across the Dampier Sub-basin showing four tectonic structures in this study. Abbreviation: SB, Sub-basin

Northwest Shelf of Australia (Longley et al., 2002; Marshall & Lang, 2013; McHarg, Elders, & Cunneen, 2019a, 2019b; Thomas et al., 2004; Figure 1a). This study focuses on the late syn-rift succession in the north-western part of the Dampier Sub-basin, the entirety of which is imaged by the Fortuna 3-D seismic survey (Figure 1a,b). In cross-section, the Dampier Sub-basin exhibits an asymmetric graben-like geometry, bounded on the west by the SE-dipping Rankin Fault System, and on the east by the NW-dipping Rosemary Fault System (Longley et al., 2002; Marshall & Lang, 2013; McHarg, Elders, & Cunneen, 2019a; Stagg, 2004; Figure 1c,d). Within the Dampier Sub-basin, the NE-SW-striking Madeleine Trend anticline separates two NE-SW-striking elongate synclinal depressions, the Lewis Trough to the southeast and the Kendrew Trough to the northwest (Figure 1b). The Rankin Platform lies in the footwall of the Rankin Fault System and was deeply eroded during the Jurassic and Early Cretaceous and acted as a sediment source to the Dampier Sub-basin (Barber, 1994; Longley et al., 2002; Marshall & Lang, 2013; Figure 1c,d).

As indicated by 2D seismic lines, the Dampier Sub-basin contains an over 10-km-thick late Paleozoic-Cenozoic succession (Jablonski, 1997; Marshall & Lang, 2013; Stagg, 2004; Figures 1d and 2). Late-Mesozoic rifting started in the Early Jurassic (Pliensbachian) and continued to the end of Early Cretaceous (Valanginian), and is interpreted to comprise three stages: (i) early syn-rift stage (J20 interval), (ii) main syn-rift stage (J30-J40 interval) and iii) late syn-rift stage (J50 interval) (Longley et al., 2002; McHarg, Elders, & Cunneen, 2019b; Stagg, 2004; Figure 2). During the early syn-rift stage, structurally high blocks developed along the Enderby Trend and Rankin Platform, with marine clays and silty sands of the Athol Formation and Legendre Formation, respectively, in the Dampier Sub-basin (Longley et al., 2002; Marshall & Lang, 2013; McHarg et al., 2019b; Figure 2). The early main syn-rift stage (Callovian to Kimmeridgian) marks continental break-up and the onset of seafloor spreading, with deposition of transgressive shallow marine sands of the Calypso Formation (McHarg et al., 2019a, 2019b; Stagg, 2004; Figure 2). Following the transgression, localized basin-floor fans of the Eliassen Formation were deposited (e.g., Fullerton,

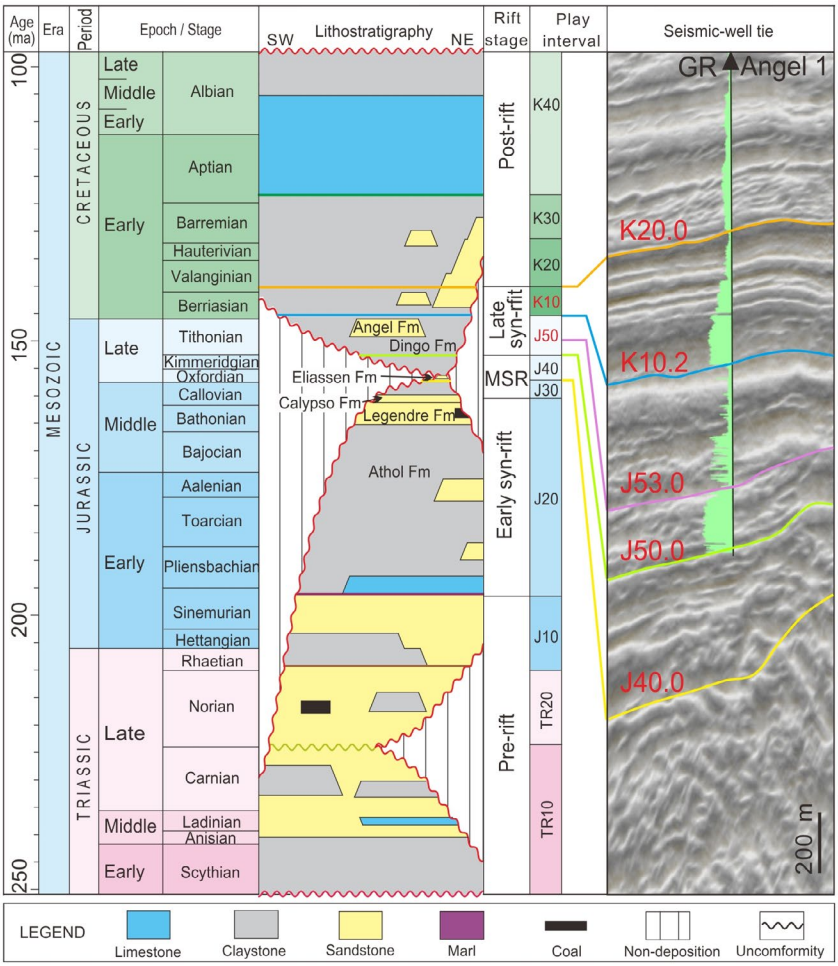

FIGURE 2 Generalized stratigraphic column for the Dampier Sub-basin with seismic-stratigraphic horizons used in this study indicated (after Stagg, 2004). Note the interval of interest in this study is the J50 interval which developed in the late syn-rift stage. Abbreviation: MSR, Main syn-rift; Fm, Formation

Sager, & Handschumacher, 1989; Hill, 1994; Stagg, 2004; Figure 2). During the late main syn-rift stage, restricted oceanic circulation was prevalent in the immediate hanging wall of the Rankin Fault System resulting in widespread deposition of the Dingo claystone (e.g., Thomas et al., 2004). During the late syn-rift stage, the Rankin Platform acted as a coarse-grained sediment source to the Kendrew Trough, where thick sandstones called the Angel Formation were deposited – the interval of interest for this study (Longley et al., 2002; Marshall & Lang, 2013; McHarg et al., 2019b; Stagg, 2004; Figure 2). After deposition of the Angel Formation, tectonic activity waned dramatically, and the offshore Northern Carnarvon Basin gradually evolved as a component of the Northwest Australian passive margin throughout the Early Cretaceous (Berriasian) to present day (Cathro & Karner, 2006; Longley et al., 2002; McHarg et al., 2019b; Figure 2).

3 | DATA AND METHODS

3.1 | Seismic data

This study utilizes full-stack seismic reflection data, the Fortuna 3-D survey, that cover an area of *ca*. 6,300 km^2, and was collected in 2014 by Woodside Energy Company and its partners. The seismic data are in the depth domain, with a line and trace spacing of 12.5 m, and images down to 10,000 m depth, which fully captures the Jurassic rift interval (Figure 3a). The seismic data are presented in reverse polarity (SEG Convention), which means that a downward increase in acoustic impedance is represented by a "trough" (red reflection in images provided). Within the stratigraphic interval of interest, the seismic data have a dominant frequency of ca. 20 Hz. Given an average ΔT of *ca*. 240 us/m within the J50 interval on sonic logs of the Angel 1 well, the average interval velocity is of *ca*. 4,200 m/s and the vertical seismic resolution is *ca*. 50 m.

3.2 | Well and core data

We used 21 exploration wells containing a suite of well-logs enabling seismic-well ties and providing key stratigraphic surfaces and sedimentological interpretations (Figure 3a). We tied stratigraphic surfaces to the seismic data and mapped these surfaces throughout the seismic data to construct a tectono-stratigraphic framework (Figure 2). This framework enables observations

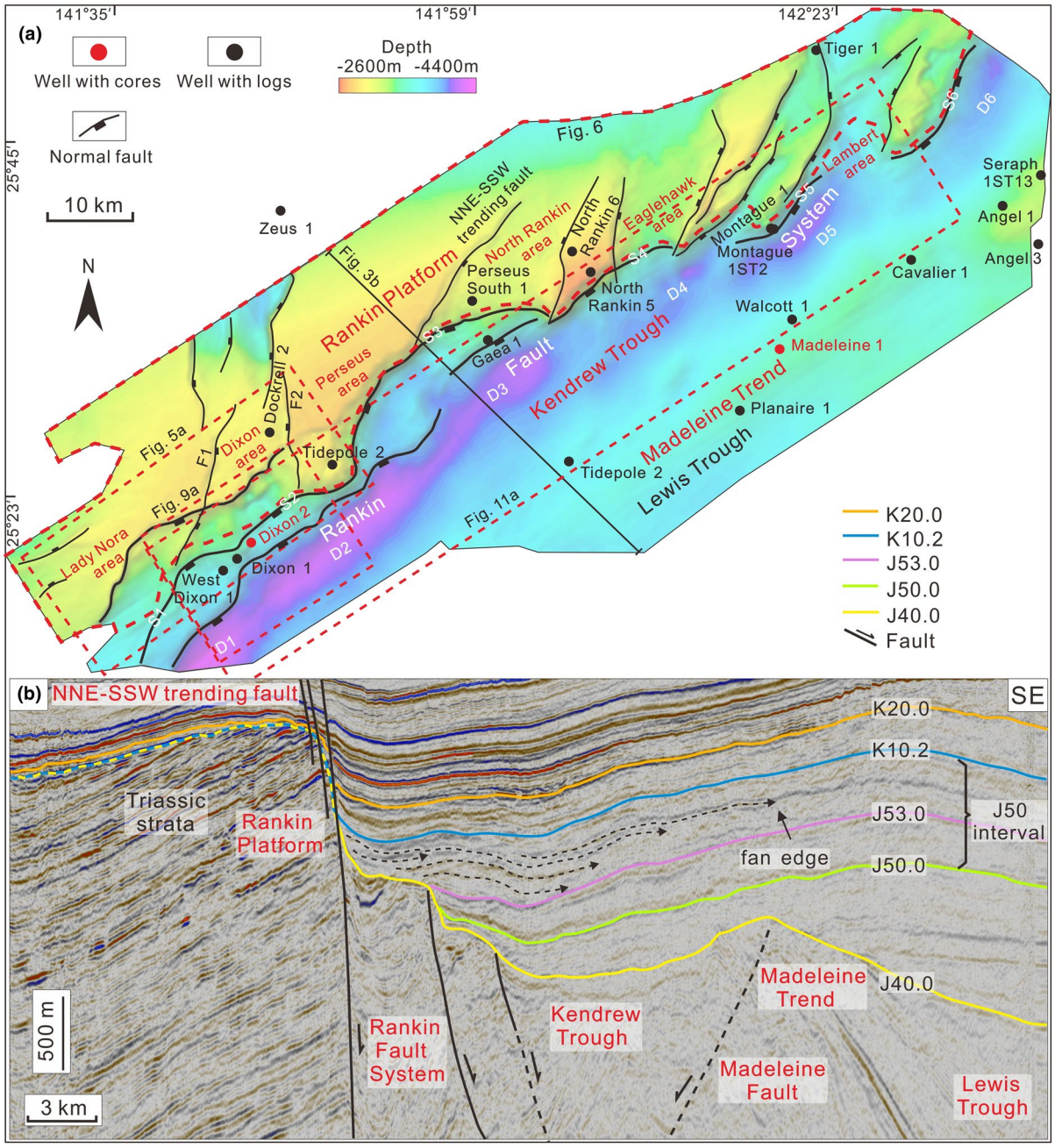

FIGURE 3 (a) Depth-structure map of the J50.0 horizon showing the configuration of structural elements in the Fortuna 3D seismic survey with detailed faults and well locations indicated. The site of this map displays in Figure 1b. (b) A seismic section cross-cutting the rift axis showing the mapped seismic horizons and the configuration of structural elements in the seismic survey. The location of the seismic section displays in (a). Abbreviation: F1, Fault 1; F2, Fault 2; S1–S6, fault segment 1–6; D1-D6, depocenter 1–6

on the temporal evolution of the basin and interpretation of the key rift stages (Longley et al., 2002; Marshall & Lang, 2013; McHarg et al., 2019b). Most of the wells on the Rankin Platform and Madeleine Trend penetrate the Jurassic strata, whereas very few penetrate the equivalent interval in the Kendrew and Lewis troughs (Figure 3a). We incorporated core from two wells, the Dixon 2 well drilled in the Kendrew Trough and the Madeleine 1 well drilled in the Madeleine Trend. These core penetrated *ca.* 100 m of the J50 interval of interest. Using these data we interpreted sedimentary facies across the study area in both core and well-logs, and we integrated these observations with seismic geomorphological analysis.

3.3 | Seismic interpretation

Seismic interpretation was performed using Petrel 2016 and GeoTeric 2017.2. For seismic geomorphological analysis in the J50 interval, five seismic horizons, J40.0

(Oxfordian), J50.0 (Tithonian), J53.0 (Tithonian), K10.2 (Berriasian) and K20.0 (Berriasian), were mapped because of their significant stratigraphic features and our ability to tie these horizons to well data (Figure 3b). Seismic horizons and faults were manually interpreted every 16 in-lines and 16 crosslines (a 200 m spacing) across the seismic survey. For areas along fault scarps of the Rankin Fault System, we interpreted every four in-lines and four crosslines (a 50 m spacing) to capture the morphology of drainage outlets (Figure 3a). The key erosional surface in this study is the J40.0 horizon which on the Rankin Platform truncates underlying Triassic strata, and in the Kendrew Trough locally truncates Early-to-Middle Jurassic strata. The J50.0, J53.0 and K10.2 horizon are only mappable in the Kendrew Trough, and merge up-dip with the J40.0 unconformity on the Rankin Platform. The younger K20.0 horizon is mappable across the entire survey (Figure 3b). The hanging wall depositional systems explored in this study mainly developed within the J50 interval, and mainly within the stratal unit bounded by the J53.0 and K10.2 horizon (Figures 2 and 3b).

3.4 | Deep-time analysis of source drainage basin

To reconstruct an ancient drainage basin, the most widely used method is to achieve a palaeo-topography map through seismic datasets (e.g., Elliott et al., 2012). Erosional phases and horizons amalgamate up-dip onto structural highs, making it hard to restore the palaeo-topography for any one particular erosion phase. Nevertheless, we can still get a relatively accurate palaeo-topography for the last erosional surface which amalgamates numerous erosional events spanning a considerable period of geological time (e.g., Sømme & Jackson, 2013; Sømme, Jackson, et al., 2013; Helland-Hansen et al., 2016).

The Rankin Platform started eroding during early syn-rift (Early Jurassic), and the erosion continued until the development of the K10.2 horizon at the end of the late syn-rift stage (Early Cretaceous) (Longley et al., 2002; Marshall & Lang, 2013; McHarg et al., 2019b). The result was the J40.0 unconformity, a long-lived erosional surface that developed from the Early Jurassic until the Early Cretaceous and which caps the Rankin Platform (Figure 3b). The depositional systems developed in the Kendrew Trough during J50 time most closely relate to the palaeo-topography on the Rankin Platform represented by the J50.0 horizon (Figure 3b).

We flattened the seismic data on the post-rift, K20.0 Horizon as a simple approximation to remove the post-depositional deformation of the deeper J50.0 horizon. The J50.0 palaeo-morphology was then used as input to the hydrology toolbox in ESRI's ArcGIS 10.5 software to extract drainage basins and quantitative geomorphic parameters for the drainage basins developed on the Rankin Platform in the footwall of the Rankin Fault System. The cross-sectional shape of drainage outlets was approximated as a regular triangle and the total cross-sectional area of this triangular space was used as a proxy for outlet cross-sectional areas (Figure 4). We also measured the spacing of regional drainage basin outlets (S) defined as the distance between the outlets of two neighbouring drainage basins parallel to the border fault (e.g., Hovius, 1996; Talling, Stewart, Stark, Gupta, & Vincent, 1997; Figure 4).

The uncertainty of this analysis of drainage basins depends on the accuracy and detail of the original J50.0 unconformity surface and how accurate the simple restoration process is. The interpretation of the J50.0 unconformity in seismic sections with a spacing of 200 m and a spacing of 50 m for drainage outlet areas along the Rankin Fault System. Based on the dominant frequency of the seismic data at the depth of interest and the interval velocity, vertical measurements have a resolution of 1/4 wavelength, or about 50 m. However, many of the horizontal measurements are collected on spatial analysis which has a resolution of *ca*. 25 m.

Although our approach to restoring the J50.0 unconformity is simplistic, it achieves a map-view restoration of footwall drainage catchments and stream networks that is comparable to many active rift basins (e.g., Leeder & Jackson, 1993; Whittaker, Attal, & Allen, 2010), allowing plan-form attribute geomorphic parameters to be measured (drainage basin area, drainage basin length, and width, length of the longest channel; Figure 4). Our restoration is, however, not appropriate for measuring cross-sectional parameters such as channel gradient.

A drainage basin whose head coincides with the rift drainage divides is considered a major footwall drainage basin (e.g., drainage basins 2 and 5; Figure 4) (e.g., Hovius, 1996; Talling et al., 1997). In contrast, drainage basins that do not extend up to the rift drainage divide and have a rill-like morphology along the fault scarps are termed local footwall drainage basins (e.g., drainage basins 1, 3, 4, and 6; Figure 4). Local footwall drainage basins drain only a minor portion of the basin's footwall, so their importance on morphology (and sediment supply) is only local. Therefore, we only focused on major footwall drainage basins (e.g., Hovius, 1996; Talling et al., 1997), but take into account all of the major and local footwall drainage basins in our analysis of scaling relationships between source and sink (e.g., Hovius, 1996).

3.5 | Geomorphological analysis of sink depositional systems

To analyze the hanging wall depositional systems, we utilized core from two wells and logs from seven wells that penetrate

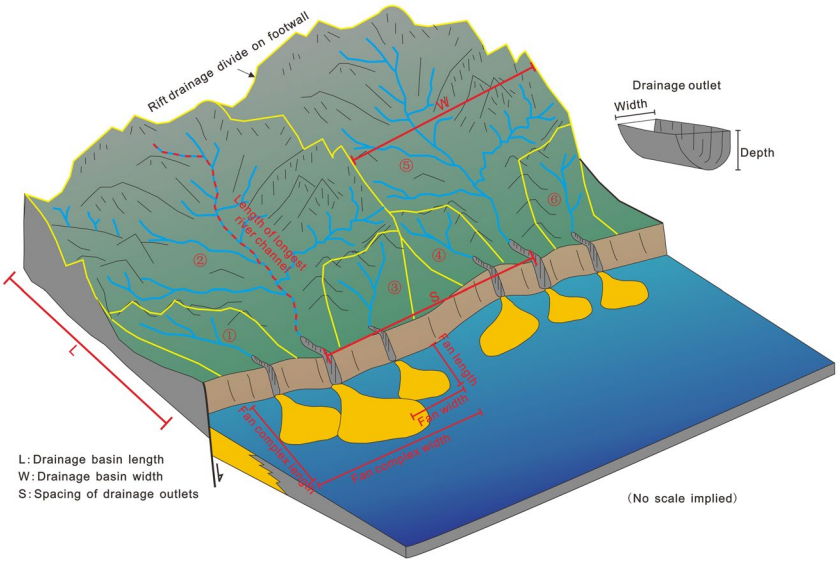

FIGURE 4 Geometric parameters about drainage basins, drainage outlets, submarine fan complexes and drainage domain that featured the source-to-sink systems in this study. Major footwall drainage basins develop drainages that headward eroded towards the drainage divide, such as drainage basins 2 and 5. Local footwall drainage basins develop rill networks along the fault scarps, such as drainage basins 1, 3, 4 and 6. Drainage basins 1, 2 and 3 share a similar tectono-geological substrate and thus we grouped them into one drainage domain (e.g., Leeder et al., 1991)

the J50 interval. Colour, lithology, sedimentary structures, grain size and trace fossils from the core were used to interpret sedimentary facies and infer depositional environments. Gamma-ray (GR) logs were also used to interpret lithology and note the vertical variations in lithology.

Geomorphic characteristics of the depositional system in the Kendrew Trough were mapped in seismic cross-sections and on planform attribute maps. The main attributes used for the sedimentological and geomorphological analysis of the depositional systems in the Kendrew Trough were spectral decomposition Red-Green-Blue (RGB) colour blends, Root Mean Square (RMS) amplitude and variance. Interpretation of attribute maps was calibrated by comparison with cross-sectional seismic facies analysis. Optimal frequency decomposition bins for RGB blending were 13 Hz (red), 18 Hz (green) and 22 Hz (blue) which spans the dominant frequency (20 Hz) in the J50 interval. Attributes were extracted on seismic stratal slices to capture clearer geomorphic features within a relatively short depth window (typically <30 m). Nineteen iso-proportional slices were generated between the J53.0 and K10.2 horizons (labelled SS1 to SS19, youngest to oldest).

The distal edges of hanging wall fans were mapped as the terminus of downlapping reflections on depositional dip-oriented seismic sections (Figure 3b), and the corresponding downlap termination positions on seismic attribute slices were noted. These terminus lines were used to calculate the width, length and area of hanging wall fans. We considered these seismic amplitudes-based measurements a minimum because of seismic resolution limitations, and the fact that the increasing finer-grained nature of fan margins decreases their reflection contrast with the fine-grained background sediments, limiting imaging of this lithologically transitional fan fringe (e.g., Chen et al., 2019; Wood, 2007). Due to the large areal extent of some submarine fans, and their often overlapping nature, it is difficult to map the full extent of the fans sourced from each drainage catchment, thus we grouped submarine fans into fan complexes that correspond to each drainage domain. For example, the fan complex labelled in Figure 4 relates to sediment exported from the drainage domain formed by drainage basins 1, 2 and 3 (Figure 4). This methodology reduces the uncertainty in geomorphologic parameters that might be caused by the over-interpretation of seismic attributes beyond the resolution of the seismic (Figure 4).

4 | STRUCTURAL FRAMEWORK OF THE NORTHWEST DAMPIER SUB-BASIN

The structural framework of the study area is best illustrated with the depth-structure map of the J50.0 horizon as it records the syn-rift deformation and topography of the rift (Figures 2 and 3). The rift topography of the J50.0 horizon was defined by the Rankin Fault System and an array of NNE-SSW-striking faults clearly imaged on the Rankin Platform (Figure 3a).

The Rankin Fault System is composed of six main segments and has a total length of about 120 km and an overall NE-SW-strike (Figure 3a). The south-western segments of the fault (S1, S2 and S3; Figure 3a) are ca. 70 km long, strike NE-SW,

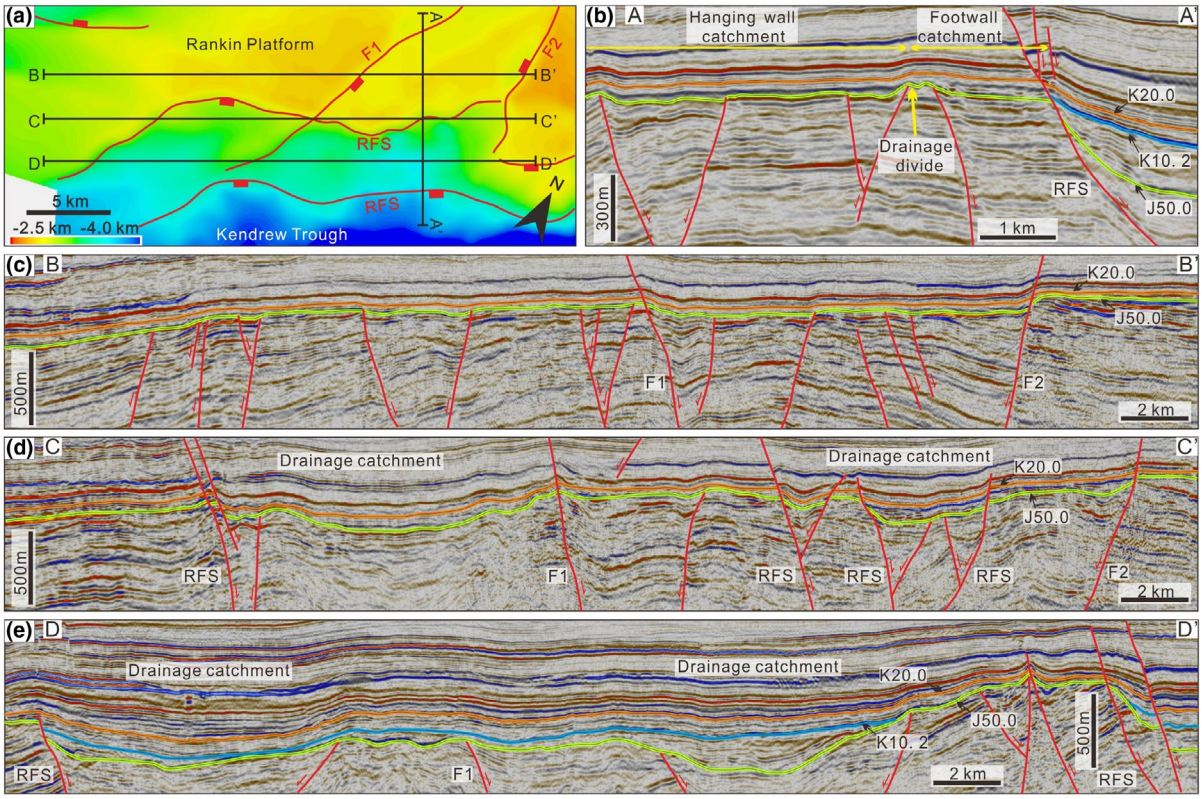

FIGURE 5 (a) Depth-structure map of the J50.0 horizon on the Rankin Platform showing the erosion features. The site of this map shows in Figure 3a. (b) Dip seismic section across the Rankin Platform showing the footwall erosion and watershed on the Rankin Platform. (c–e) Seismic sections along the strike of Rankin Platform showing the topography changes approaching the Rankin Fault System. The sites of seismic sections display in (a). Abbreviation: RFS, Rankin Fault System; F1, Fault 1; F2, Fault 2

dip to the SE and have an average displacement of *ca*. 730 m. These fault segments bound the deepest depocenters in the south-western Kendrew Trough and are typical *ca*. 55 km long and *ca*. 9 km wide (D1, D2, and D3; Figure 3a). The north-eastern segments (S5 and S6; Figure 3a) strike NNE-SSW and dip to the *SSE*, with lengths ranging from 14 to 16 km, and an average displacement of *ca*. 700 m. These segments control the development of two smaller depocenters which are each *ca*. 15 km long and *ca*. 6 km wide (D5 and D6; Figure 3a).

In cross-section, the Rankin Fault System appears to be basement rooted and has an upper fault tip commonly located in lowermost Cretaceous strata (Figures 1d and 3b). As shown in the dip seismic section, the J50 interval develops a broadly tabular cross-sectional geometry, with no major growth packages into the immediate hanging wall, suggesting relatively little activity along the Rankin Fault System during this time interval. Triassic strata on the Rankin Platform beneath the J50.0 horizon tilt towards the northwest, indicating activity on the Rankin Fault System prior to J50.0 (Tithonian) time was accommodated primarily by footwall uplift and back-tilting (Figures 1d and 3b). The footwall stratigraphy of the K10 interval on the Rankin Platform contains sub-parallel, medium-continuity seismic reflections (Figure 3b), suggesting there was no significant footwall uplift or back-tilting on the Rankin Fault System after deposition of the J50 interval.

The array of NNE-SSW-striking faults on the Rankin Platform created a series of NNE-SSW-trending grabens, half-grabens and horst blocks (Figure 3a). The strike of these faults swings clockwise from nearly N-S-striking in the southwest to NE-SW-striking in the northeast (Figure 3a). In cross-section, these faults are planar, with their lower tips mostly located in Upper Triassic strata, and their upper tips in lowermost Cretaceous or uppermost Triassic strata (Figures 1d, 3b and 5). As most Jurassic sediments on the Rankin Platform have been eroded, it is hard to tell whether these faults had any activity during the Jurassic rift phase.

5 | GEOMORPHOLOGY OF FOOTWALL DRAINAGE ALONG THE RANKIN FAULT SYSTEM

5.1 | Geomorphological analysis and development of drainage basins

The development of footwall drainage basins is associated with the rifted topography in the footwall of the Rankin

Fault System and the subsidiary NNE-SSW-trending faults (Figure 5). Drainage basins gradually widen and deepen as one moves from the drainage divide to drainage outlet (Figure 5c–e). The drainage basins are mostly located within NNE-SSW-trending grabens and half-grabens. However, depth of the drainage basin, and thickening of younger sedimentary infill, is largely due to incision of drainages into the underlying strata, rather than activity on the NNE-SSW-trending faults (Figure 5c–e).

A total area of about 1,900 km^2 of the Rankin Platform supplied eroded Triassic and Jurassic sediments southeastward, across the Rankin Fault System, into the Kendrew Trough (Figure 6a,b), and north-westward drainages flowing into the Exmouth Plateau during the Late Jurassic to Early Cretaceous (Figures 1b and 6a). Southeast-directed drainages are separated from the northwest-directed drainages by the main rift drainage divide (Figure 6b). The 24 individual footwall drainage basins that supplied sediment to the Kendrew Trough occupy about one third of the area of the Rankin Platform and extend up to 11 km into the footwall of the Rankin Fault System (Figure 6a and b).

Geomorphological analysis shows that drainage basins with a dendritic drainage pattern (e.g., drainage basin 3, 8 and 22; Figure 6b) usually have relatively smaller aspect ratios (about 0.45 to 0.8) compared to those with a linear drainage pattern (e.g., drainage basin 9, 14 and 24; Figure 6b). The length of the longest channel within each drainage basin shows a strong positive correlation to the area of the drainage basin, supporting the validity of this hydrological analysis as an accurate representation of the distribution of drainage basin boundaries and the plan-form geometry of drainage basins (Figure 7a). Furthermore, the spacing of drainage outlets along the Rankin Fault System displays a moderately strong, positive, linear relationship to the drainage basin length (Figure 7b), which is similar to that proven for present-day linear mountain belts (Hovius, 1996) and linear fault blocks (Talling et al., 1997).

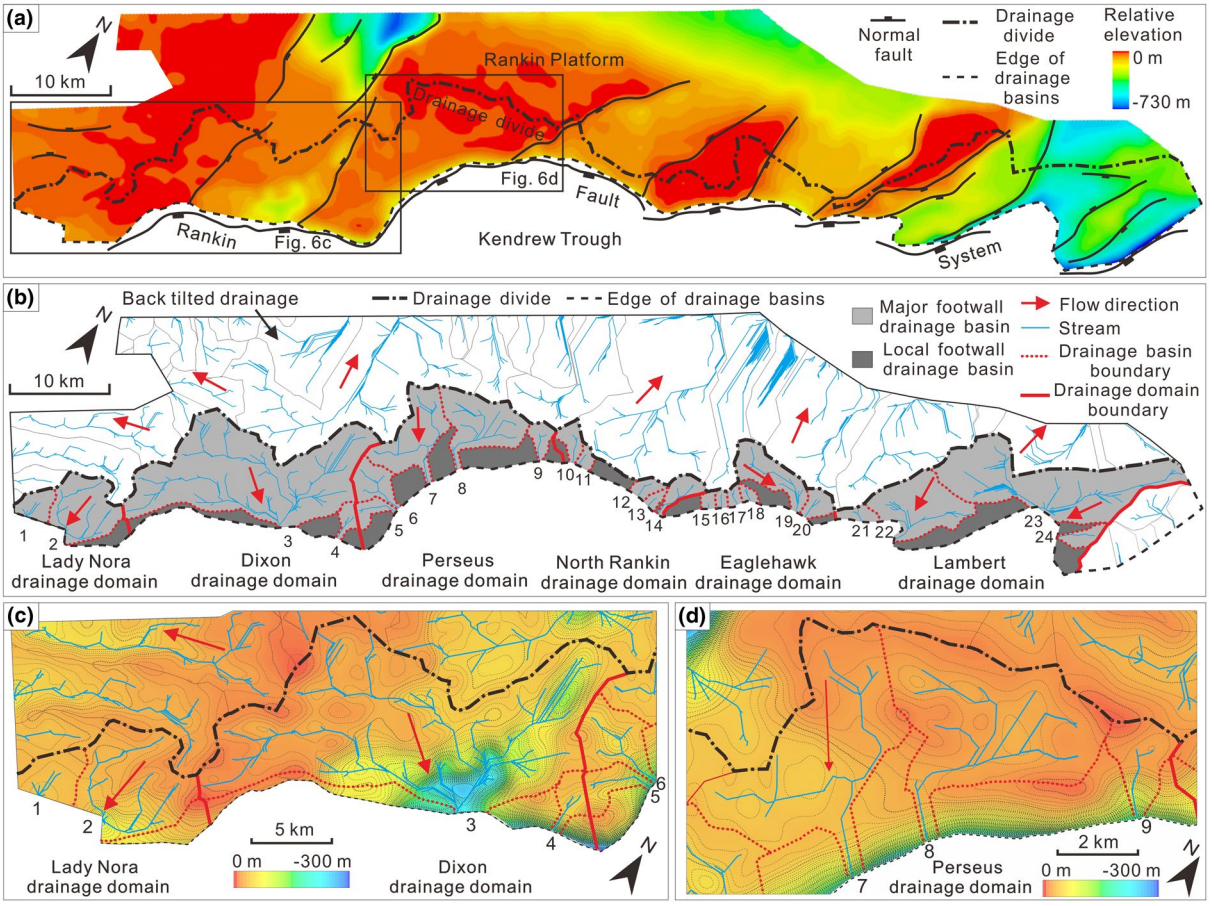

FIGURE 6 (a) K20 flattened depth-structure map of the J50.0 horizon defining the drainage basins on the Rankin Platform. (b) Plainview area of drainage basins on the Rankin Platform with drainages for each drainage basin highlighted. Light grey colour drainage basins are major footwall drainage basins that head on the rift drainage divide, as well as the main drainage domains. Dark grey colour drainage basins are local footwall drainage basins (see more text for discussion). (c–d) Details of the morphology of the Dixon and Perseus drainage domains

5.2 | Geomorphological analysis of drainage domains and drainage outlets

The 24 drainage basins along the Rankin Fault System can be further grouped into six major drainage domains based on a similarity of their tectonic and geological elements (e.g., Duffy et al., 2015; Leeder, Seger, & Stark, 1991; Figure 6b and Table 1). Four of these drainage domains, Dixon, North Rankin, Eaglehawk and Lambert, are situated over NNE-SSW-trending grabens on the Rankin Platform (Figure 6a,b). In contrast, Lady Nora and Perseus drainage domains are developed on a horst between parallel NNE-SSW-trending faults (Figure 6a,b). The boundaries of all six drainage domains are mostly defined by NNE-SSW-striking faults that abut the Rankin Fault System (Figure 6). The drainage outlets for each of these domains are relatively well preserved on the Rankin Fault System scarp (Figure 8a). These drainage outlets cut down into the underlying Triassic strata and are filled with younger strata, mostly of K10.2 interval age (Berriasian), that onlaps their outlet walls (Figure 8b,c). In the following sections, we describe representatives of the two categories of drainage domains; the Dixon drainage domain within a NNE-SSW-trending graben and the Perseus drainage domain on a NNE-SSW-trending horst.

5.2.1 | Dixon drainage domain

The Dixon drainage domain occupies an area of *ca*. 156 km^2 and is mostly confined within a 26-km-wide, 11-km-long graben in the footwall of the Rankin Fault System that is oriented parallel to the Rankin Fault System (Figure 6a,c). In detail, the drainage domain has a dendritic planform and comprises three major channel branches that are oriented roughly N–S, perpendicular to the Rankin Fault System in their lower reaches, but become sub-parallel to the Rankin Fault System towards the head of the drainage domain (Figure 6c). On seismic data, 12 drainage outlets are mappable along the footwall scarp, with widths ranging between 480 m and 2,145 m and an average depth of *ca*. 31 m (Figure 8a and Table 1). The main drainage outlet locates to the northeast of this drainage domain, with a width and depth of *ca*. 1,526 m and *ca*. 46 m respectively (Figure 6c and Table 1).

5.2.2 | Perseus drainage domain

This drainage domain covers *ca*. 120 km^2 and mostly occurs on a horst block (Figure 6a,d). The maximum distance to the rift drainage divide is *ca*. 9 km and parallel to the fault, the drainage

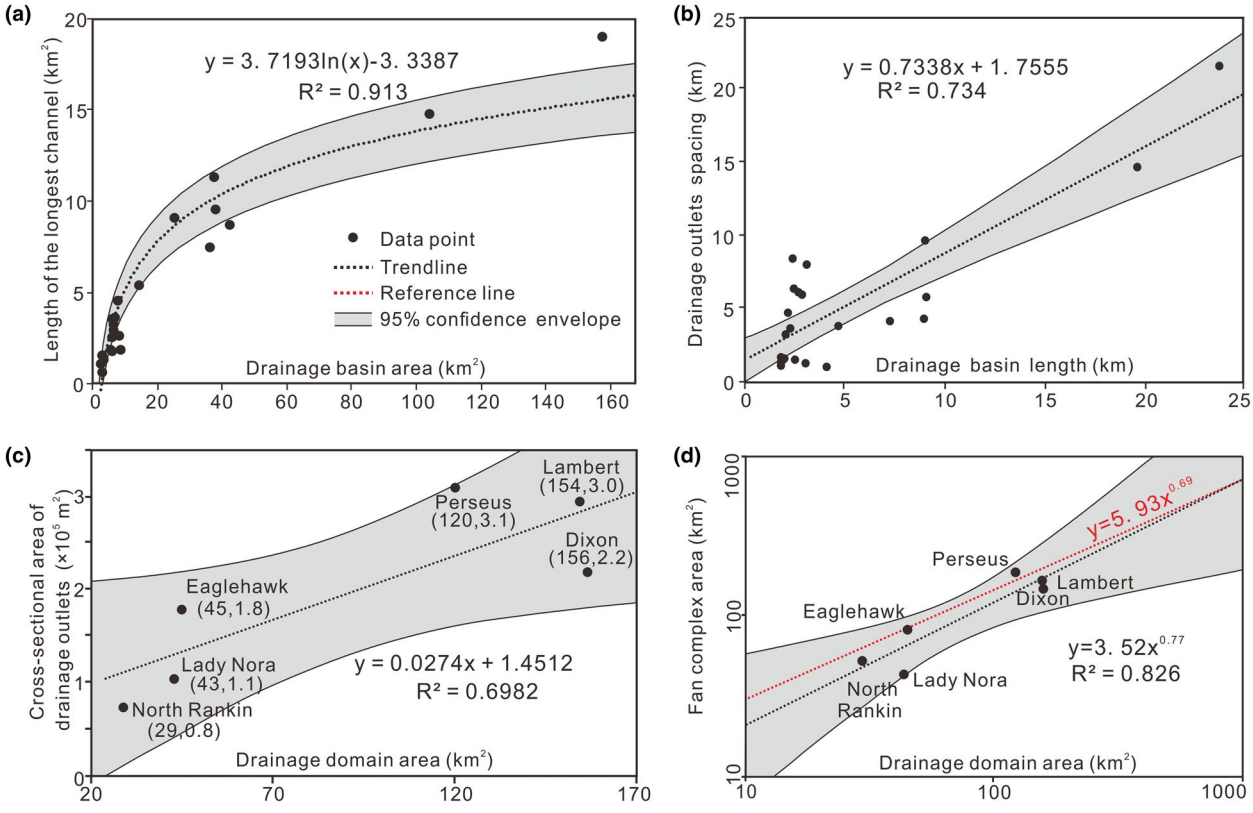

FIGURE 7 Source-to-sink geomorphic parameter relationships for the Rankin Platform and Dampier Sub-basin. (a) Drainage basin area versus length of the longest channel. (b) Drainage basin length versus drainage outlets spacing. (c) Drainage domain area versus drainage outlets cross-sectional area. (d) Drainage domain area versus transverse submarine fan complex area for six source-to-sink systems. The Redline is the general relationship from Nyberg et al. (2018)

TABLE 1 Quantitative analysis of the drainage domain area and cross-sectional area of drainage outlets

District	Drainage domain area (km^2)	The cross-sectional area of drainage outlets ($\times 10^5$ m^2)	Submarine fan complex area (km^2)	The geometry of drainage outlets											
				Width (m) top											
				Depth (m) below											
				1	2	3	4	5	6	7	8	9	10	11	12
Lady Nora	43	1.1	43	2,176	1,526	858	927								
				39	48	41	20								
Dixon	156	2.2	146	1,562	2,145	1,200	873	961	1,528	1,660	994	480	1,046	1,526	709
				30	24	28	24	29	23	27	26	25	38	46	38
Perseus	120	3.1	193	1,205	1,797	1,806	1,998	887	1,109	629	703	724	659	813	
				79	87	34	50	37	46	32	27	43	53	22	
North Rankin	29	0.8	52	779	1,208	1,406									
				27	39	58									
Eaglehawk	45	1.8	83	2,090	2,123	443	470	427	1,237	1,599	3,196	796	393		
				34	57	15	25	24	28	14	21	15	20		
Lambert	154	3.0	163	2,874	2,069	1,035	3,821	1,685	1,716						
				83	56	16	24	38	36						

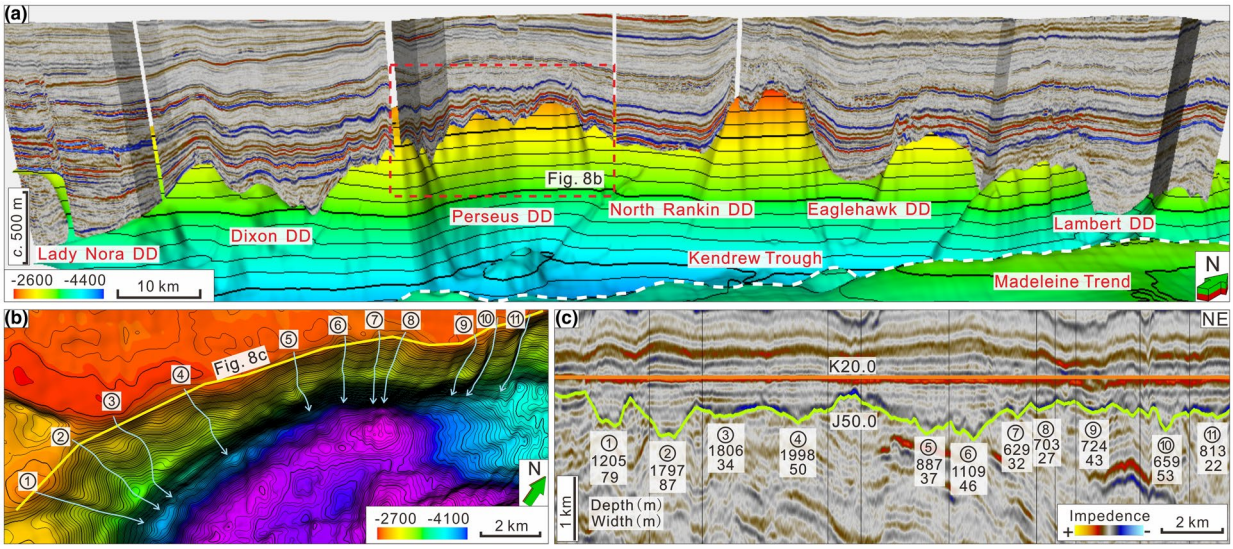

FIGURE 8 (a) Perspective view of the seismic sections along the strike of Rankin Platform showing the distribution of drainage outlets for each drainage domain on the J50.0 horizon. Abbreviation: DD, drainage domain. (b) Closer view of 11 drainage outlets that developed along the edge of the Perseus drainage domain. (c) The geometric measurements of drainage outlets in the Perseus drainage domain. The site of this seismic section is shown in (b) in the yellow line

domain has a maximum width of *ca*. 22 km (Figure 6a,d). Within this drainage domain, "mushroom"-shaped drainage basins are oriented broadly NW-SE, with dendritic channels that flowed to the southeast, perpendicular to the Rankin Fault System (Figure 6d). Instead of converging to a single, major channel at the scarp of the Rankin Fault System as seen in the Dixon drainages, drainages in these "mushroom"-shaped drainage basins flow out of the drainage domain independently (Figure 6d). Eleven separate drainage-basin outlets are mappable along the footwall scarp with widths ranging from 629 m to 1,998 m and an average depth of *ca*. 46 m (Figure 8b and Table 1).

6 | SEDIMENTOLOGICAL AND GEOMORPHOLOGICAL ANALYSIS OF DEPOSITIONAL SYSTEMS IN THE KENDREW TROUGH

Two primary depositional systems comprise the terminal depositional systems in the Kendrew Trough, transverse submarine fan systems and axial turbidite channel systems.

6.1 | Sedimentological analysis of depositional systems in the Kendrew Trough

6.1.1 | Transverse Submarine fan systems

Description

Within the J50 interval, seismic sections oriented parallel to depositional dip show low-amplitude, low-continuity, low-frequency progradational, downlapping seismic reflections that form several units up to *ca*. 250 m thick with a lensoid shape, and extend *ca*. 5,500 m into the hanging wall, away from the Rankin Fault system (Figure 9a,b). The basal surface of these lensoid seismic facies is a medium-to-high amplitude reflection of medium-to-high continuity that is conformable with the underlying reflections. The top surface is a medium- to low-amplitude, low-continuity reflection that is onlapped by overlying reflections (Figure 9b). In seismic sections parallel to the strike of the Rankin Fault System, this seismic facies has a mounded shape with widths that average 10 km (Figure 9c).

The center of one of these mounds is located near the Dixon 2 well and gamma-ray profiles in the J50 interval show bell, cylindrical- and blocky shapes, 15–20 m thick, that are interbedded with thin (*ca*. 5 m) high gamma intervals (Figure 9d). Within the depth domain 3,534–3,544 m of the Dixon 2 well, the bell-shaped log facies correspond, in the core, to poorly sorted thick units of massive, light gray-coloured, fine- to medium-grained sandstone (Figures 9d and 10). The massive sandstone units mostly show a fining-upward grain-size trend with an abundance of dewatering pipes, siltstone pebbles and clay clasts, resulting in rather chaotic features in core (Figure 10). Deformed, dark-coloured bioturbated mudstones correspond to the high gamma intervals (Figure 10).

Interpretation

The core, logs and seismic inform an interpretation of these deposits as a series of submarine fans that were sourced from the Rankin Platform. The low-amplitude, low-continuity and

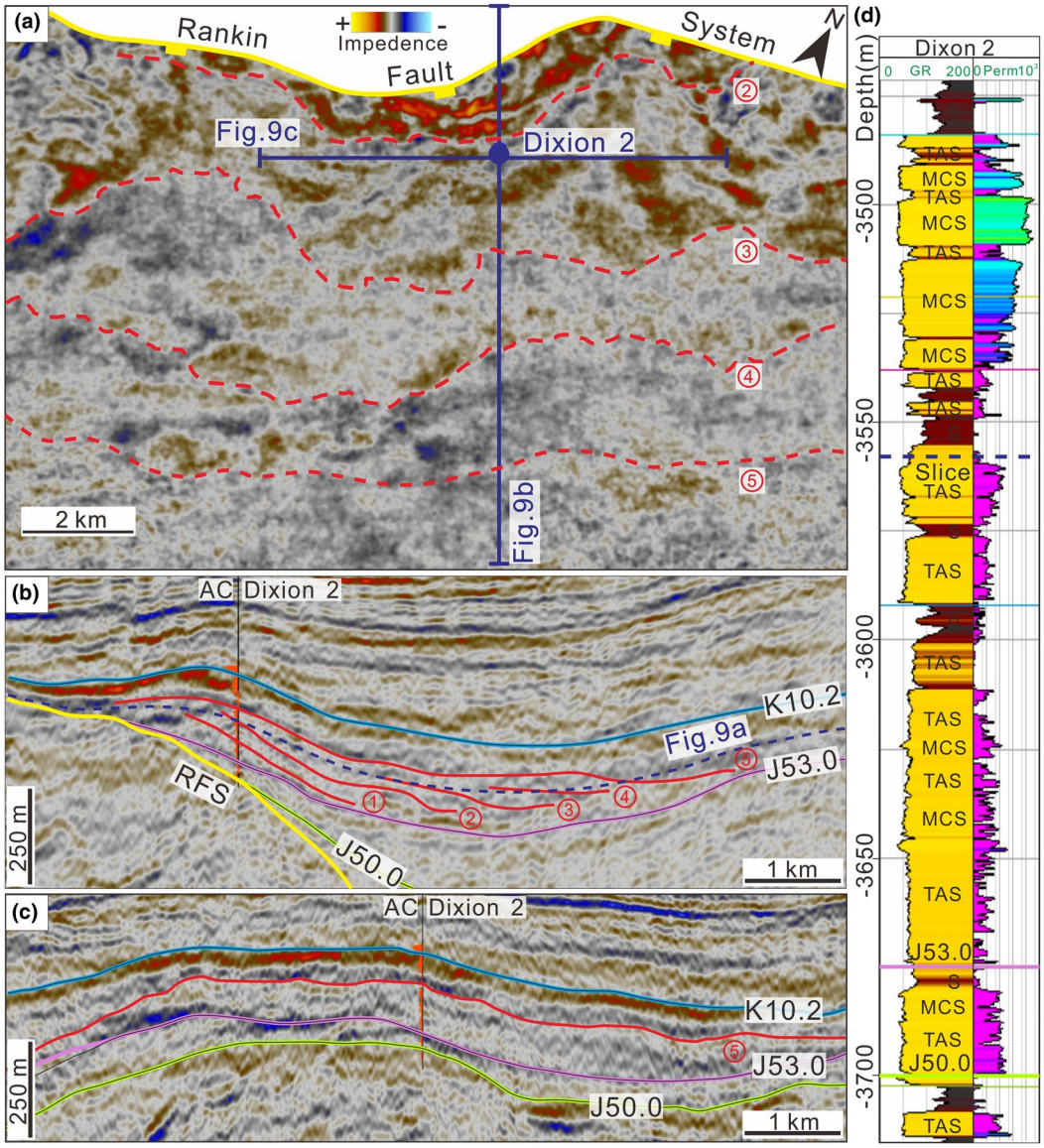

FIGURE 9 (a) Amplitude extraction of a 30 m window by stratal slicing between K10.2 and J53.0 surfaces in the Kendrew Trough. Dotted red lines refer to the boundary of fans that deposited in different phases. The location of this map is shown in Figure 3a and the depth of this seismic slice is shown in (b) as the dotted blue line. (b) The seismic section in dip direction showing progradational fans. The location of this seismic section is shown in (a). (c) Seismic section across the well Dixon 2 in the striking direction of the Rankin Fault System. The location of this seismic section is shown in (a). (d) Gamma-ray log and permeability log of well Dixon 2 showing the lithology of submarine fans in the J50 interval. Abbreviation: S, shale; MCS, mass clean sandstone, TAS, Argilacesous sandstone with traction structure. The well site can be found in Figure 3a

low-frequency seismic reflections suggest poorly bedded, poorly continuous or poorly sorted deposits, indicative of a relatively rapid depositional process. The progradational nature of the seismic reflections in this interval indicates aggradation and progradation of fan- or deltaic-style deposition. The mounded top surface and flat basal surface indicate a relatively flat depositional topography away from the adjacent fault scarp. The chaotic sedimentary features of the massive sandstone units in this interval support the interpretation of these sediments that were deposited rapidly and we interpret these deposits as debris flows deposited in the proximal parts of the submarine fan. The mounded top surface and radial downlapping of internal seismic reflections support an interpretation of subaqueous base-of-slope submarine fans. The interbedded marine mudstone supports the interpretation of a deep-water, submarine in origin.

6.1.2 | Axial turbidity channels

Description

Low-sinuosity ribbon-shaped amplitudes are present in planform RMS amplitude and RGB attribute maps within the J50 interval. This seismic facies extend *ca*. 92 km parallel to the

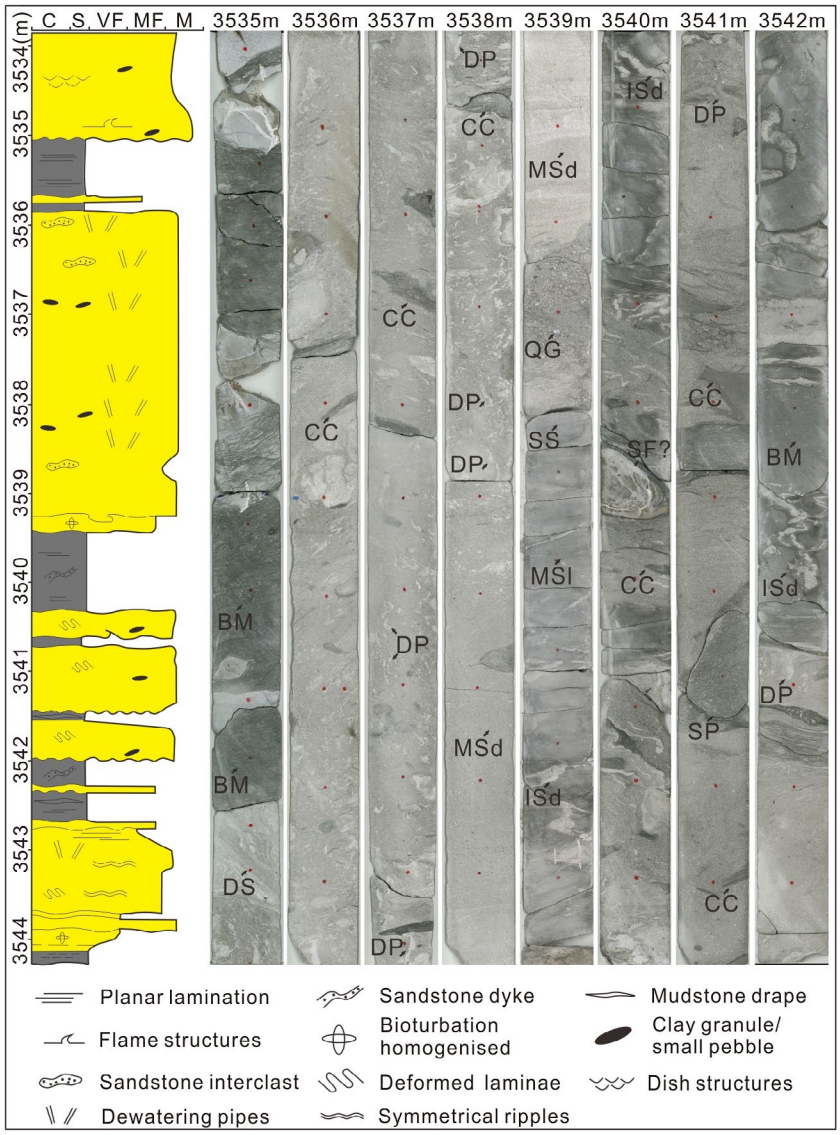

FIGURE 10 Summary sedimentological log of core from well Dixon 2 at the base of the upward coarsening succession (see Figure 9d for depth) with 1-m core stick photographs highlighting examples of sedimentary structures. The sedimentological log is reproduced after Dixon 2 well-completion report by Woodside (2007). Core photos from Geoscience Australia (www.ga.gov.au). Abbreviations: DP, dewatering pipes; ISd, injected san dykes; BM, bioturbated mudstone; CC, clay clasts; SP, siltstone pebbles; SF, slump fold; MSI, massive siltstone; SS, scour surface; QG, quartz granules; MSd, Massive sandstone; DS, dewatered sandstone

axis of the Kendrew Trough, and are located between 1.5 and 4.0 km away from the trace of the Rankin Fault System (Figure 11a,b). In dip-oriented seismic sections, the ribbon-shaped amplitudes correspond to units of medium-amplitude, medium-continuity, and low-frequency, concave up, channel-shaped seismic reflections (Figure 11b–g). The width of these individuals, channel-shaped amplitude "pods" ranges from 1.2 to 4.3 km, with thicknesses ranging from 30 to 150 m (Figure 11c–g). The axial channel-shaped seismic reflections appear to be either synchronous with or immediately post-date the oldest phases of the transverse submarine fans within the lower portions of the J50 interval (just above the J53.0 horizon) (Figure 11c–g). Subsequent transverse submarine fans downlap on this oldest phase of submarine fans and associated channel-shaped seismic reflections. Unfortunately, no wells penetrate the channel-shaped seismic reflections in the Kendrew Trough.

Interpretation

The development of the low-sinuosity ribbon-shaped, channelized seismic facies offset 1.5 to 4.0 km into the hanging wall of the Rankin Fault System suggests the development of a NW-SE-trending depositional system parallel to the rift axis. The cross-sectional channel-shaped reflectors and their planform low-sinuosity, ribbon geometry suggest channel-style erosion and deposition, which could be either fluvial or submarine in origin. These patterns occur distal to, and interfinger with, the transverse submarine fans, therefore supporting a submarine origin, and likely development through gravity-driven density flow processes (Figure 11a,b). The channel-like features are interpreted to be turbidity channels that develop along the axis of the Kendrew Trough. The trimming or cross-cutting contact with the oldest submarine fans indicates at least a part of the transverse submarine fan toes are truncated and reworked by the axial turbidity channels. (Figure 11c–g).

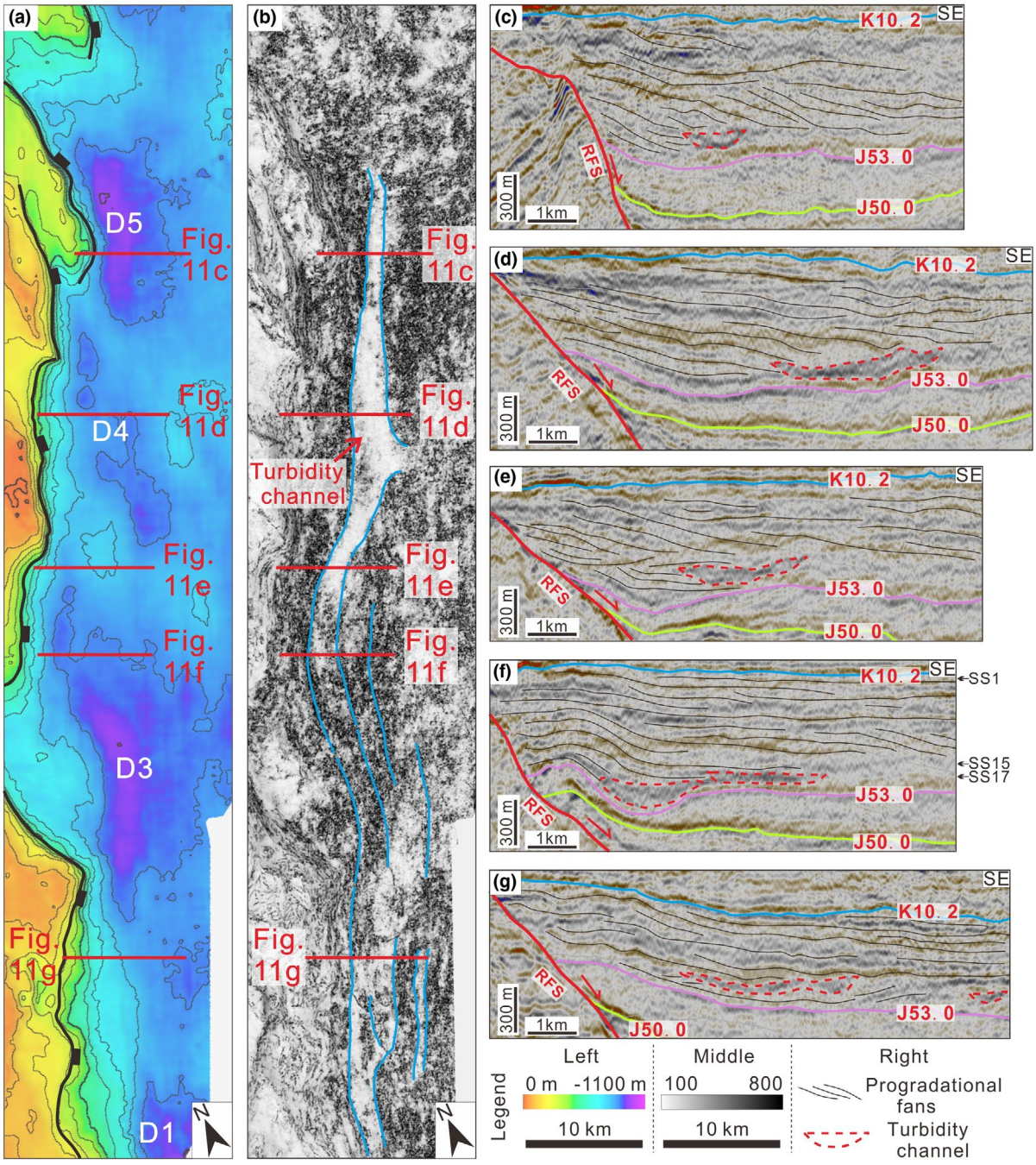

FIGURE 11 (a) K20 flattened depth-structure map of the J53.0 horizon showing the approximate palaeo-morphology in the Kendrew Trough. See Figure 3a for location. (b) Interpreted variance map between seismic slice 15 (SS15) and seismic slice 17 (SS17) showing the features of turbidity channels. Note the location of this map is the same as (a). (c–g) Interpreted seismic sections showing the temporal and spatial relationship between submarine fans and axial turbidity channels. The location of seismic sections refers to both in (a) and (b). Note the geomorphic of submarine fans and axial turbidity channels are related to the palaeo-morphology of the J53.0 horizon. Abbreviation: RFS, Rankin Fault System; D1–D5, depocenter 1–depocenter 5

6.2 | Geomorphological analysis of transverse and axial depositional systems in the Kendrew Trough

Six transverse submarine fan complexes are identified in the immediate hanging wall of the Rankin Fault System and each fan complex is spatially linked to the drainage outlets of the drainage domain on the Rankin Platform, as shown on the J50.0 palaeo-morphology map and RMS amplitude map between seismic slice 15 (SS15) and the J53.0 horizon in the Kendrew Trough (Figures 6 and 12a). The submarine fan complexes have widths, parallel to the Rankin Fault System, ranging from *ca*. 9 to *ca*. 22 km and they extend *ca*. 4 to *ca*. 9 km into the Rankin Fault System's hanging

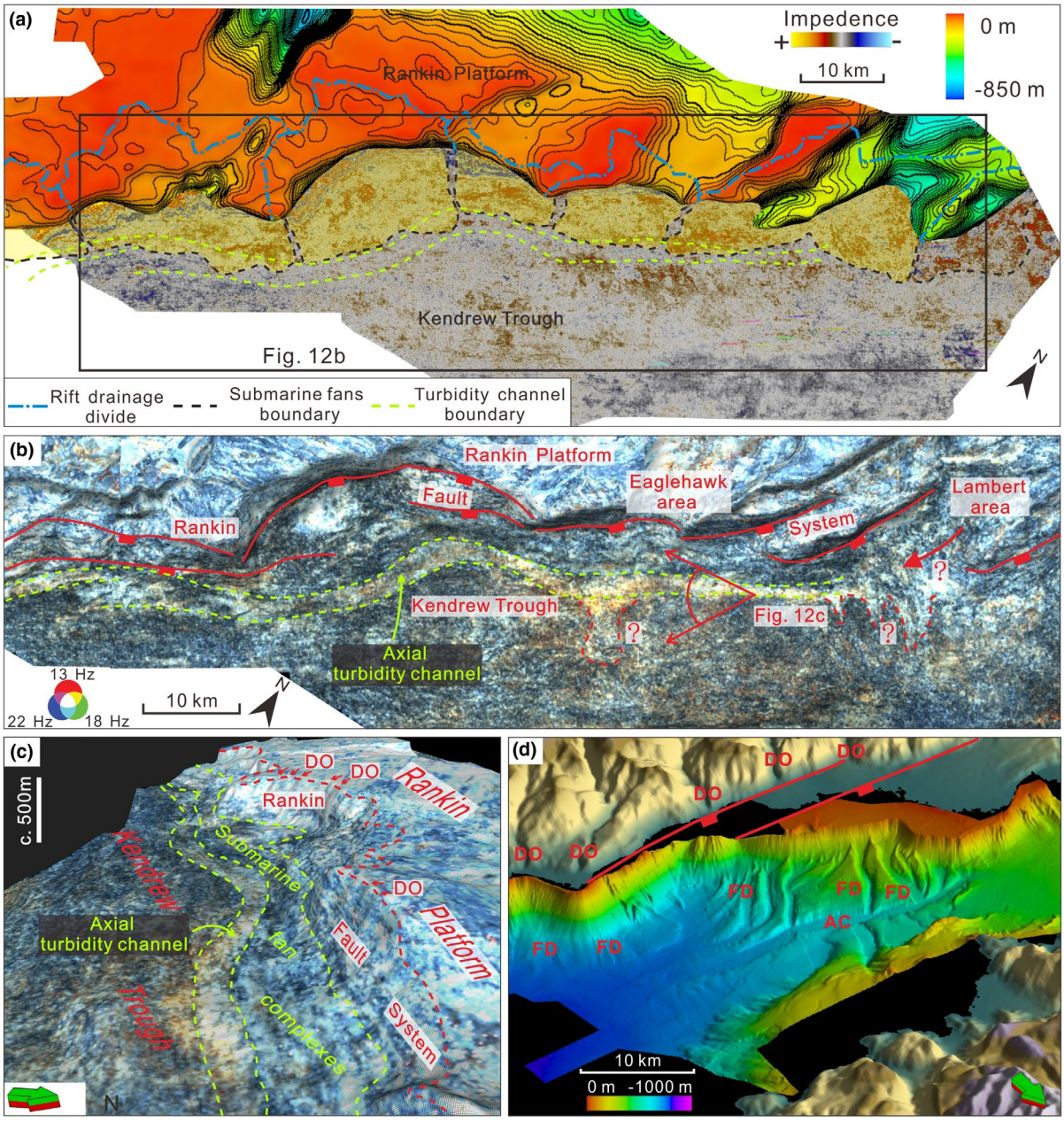

FIGURE 12 (a) Interpreted RMS attribute map covering the immediate hanging wall in the J50 interval, together with the restored palaeomorphology of the J50.0 horizon on the Rankin Platform. The RMS attribute map was calculated between the seismic slice 15 (SS15) and the J53.0 horizon. The location of SS15 is shown in Figure 11f. The dotted black lines mark the edge of seismic geomorphologies of submarine fan complex in the Kendrew Trough, and dotted yellow-green lines mark the turbidity channel boundary which depicted from (b). The dotted blue lines refer to the rift drainage divide in Figure 6a. (b) 3D view of spectral decomposition RGB blends on the seismic slice 17 (SS17) with a depth window of 30 m showing an axial turbidity channel developed in the immediate hanging wall of the Rankin Fault System. (c) A perspective view showing the turbidity channel trims the toe part of submarine fans in the Kendrew Trough. The view direction is shown in (b). (d) The basin floor of the present-day Gulf of Corinth, Greece and are interpreted to result from deflection of transverse fed turbidity currents axially along the basin towards the deepest part of the basin floor. Bathymetry data from McNeill et al. (2005). Abbreviation: DO, drainage outlet; FD, lower slope of fan delta; AC, axial turbidity channel

wall. Fan areas range from *ca*. 43 to *ca*. 193 km^2 (Figure 12a and Table 1). Submarine fans immediately above the J53.0 horizon prograde a different distance, ranging from *ca*. 1.8 to *ca*. 7.5 km, into different depocenters in the Kendrew Trough, with fan thickness ranging from *ca*. 200 to *ca*. 350 m (Figure 12), whereas younger submarine fans downlap to these older submarine fans with lengths ranging from *ca*. 3.3 to *ca*. 7.5 km (Figure 12). Furthermore, the edge of the

individual transverse submarine fan complexes forms a linear rim which trends mostly parallel to the strike of the Rankin Fault System (Figure 12).

The axial turbidity channels seem to originate from areas near the terminal end of the Lambert drainage domain in the north-eastern region of the rift and extend south-westward along the Kendrew Trough to the depocenter basinward of the Lady Nora drainage domain (Figures 6b and 12b). The width and depth of the axial turbidity channels vary on different topographies, with channels within the D5 depocenter being relatively narrow (*ca*. 1.2 km) and deep (*ca*. 100 m) (Figure 11a–d,f), whereas channels out of the D3 depocenter being wider (*ca*. 3.5 km) and shallower (*ca*. 60 m) (Figure 11a,b,e,g). The axial turbidite channel seismic facies occurs continuously in the topographic lows along the axis of the Kendrew Trough parallel to the Rankin Fault System (Figure 12b). The exception to this observation is some south-eastward extending attribute anomalies, such as in the D4 and D5 depocenters, that cross-cut more continuous features associated with the axial submarine channels (Figures 11a and 12b).

We interpret the transverse submarine fan complexes to have been toe trimmed by gravity flows entering from the northeast, before the flows reoriented to flow south-westward, parallel to the rift axis towards the deepest depocenter in the south-western Kendrew Trough (Figure 12c). The submarine erosion and redistribution of sediments associated with these axial currents occur across a distance of ca. 90 km within the study area (Figure 12a,b). There are strikingly similar process interactions occurring on the basin floor of the present-day Gulf of Corinth, Greece. There faulted topographic lows control the location of axial turbidity channels (McNeill et al., 2005). The axial turbidity channels in the Gulf of Corinth cut the toes, or distal edges of transverse fans, forming a linear margin to the transverse fan deposits around the southern, active fault-controlled basin margin (McNeill et al., 2005; Figure 12d).

7 | DISCUSSION

Integrated analysis of core, wireline log and 3-D seismic data covering the footwall and hanging wall of the Rankin Fault System has allowed a reconstruction of the full, Late Jurassic, source-to-sink system active in the late syn-rift phase of the Dampier Sub-basin, Northwest Shelf of Australia. We have shown that, in the footwall of the Rankin Fault System, Late Jurassic erosion of the Rankin Platform created a network of drainage catchments that extend headward, up to 11 km from the Rankin Fault System and supplied sediment to its hanging wall, the Kendrew Trough. The contemporaneous immediate hanging wall depositional systems comprise deep-water, transverse submarine fan complexes, sourced from individual footwall drainage domains. These transverse submarine fan complexes have a complex interrelationship with an outboard, axial turbidite channel depositional system running from northeast to southwest along the axis of the Kendrew Trough.

In this section, we discuss some of the implications of our deep-time, source-to-sink analysis that are applicable to other ancient rift basins and that also have wider application to deep-time source-to-sink studies in general. Firstly, we discuss how our approach and results help in the reconstruction of drainage basin morphology where source areas are not preserved. Secondly, we investigate the scaling relationships between segments of source-to-sink systems where there is not a simple, one-to-one relationship between a single catchment-transverse depositional system and sediment routing involves significant axial transport.

7.1 | Reconstructing source dimensions from basin margin drainage outlets

Recent source-to-sink studies of modern systems have suggested that the size of drainage basins and their associated drainage elements can strongly influence the nature and size of associated fan systems (e.g., Nyberg et al., 2018; Sømme et al., 2009; Sømme & Jackson, 2013; Sømme, Jackson, et al., 2013). Such scaling relationships, however, can be difficult to prove and apply in ancient systems since source drainage regions are often eroded during subsequent basin evolution, or if still intact, maybe poorly imaged in the subsurface (e.g., Helland-Hansen et al., 2016; Matenco & Andriessen, 2013; Sømme et al., 2009; Wu et al., 2015). However, the location of these outlets in the lower portions of the drainage system enhances the possibility that 3-D seismic data, typically being collected to image basin sinks, might image their profiles.

Studies of modern drainage systems have noted that drainage outlet morphology can provide insight into the geomorphological and sedimentological processes operating in their associated drainage basins (e.g., Hovius, 1996; Talling et al., 1997; Walcott & Summerfield, 2009). Hovius (1996) and Talling et al. (1997) demonstrated that a linear relationship exists between the spacing of drainage outlets and the length of drainage basins. In this study of the Dampier rift basin, similar scaling relationships exist between the drainage outlet spacing and the distance from the Rankin Fault System to the rift drainage divide (Figure 7b).

Whereas the value of drainage outlet spacing in reconstructing drainage basin dimensions is relatively well understood, the use of drainage outlet dimension has received less attention. Milliman and Syvitski (1992) and Hovius (1996) state that the size of fluvial systems within a drainage basin is well known to strongly influence the geomorphology and

sediment output of a drainage basin. Blum, Martin, Milliken, and Garvin (2013) suggested a relationship between the geometry of the channels in a fluvial system and its drainage area, and studies of modern, small coastal plain drainages show a strong positive relationship between drainage basin area and valley cross-sectional area (Ethridge et al., 2005; Mattheus & Rodriguez, 2011, 2014; Mattheus et al., 2007). Although there are only a few drainage domains mapped along the Rankin Platform, drainage outlet cross-sectional area along the Rankin Fault System and drainage domain area also show a positive correlation (Figure 7c). Despite the uncertainties associated with measurements from seismic data, and the timing of outlet formation compared to sink stratigraphy, as well as post-depositional modification of the outlet (e.g., during post-rift transgression), the observations from the Rankin Platform suggest that using a combination of drainage outlet spacing and cross-sectional area can provide important constraints on source area dimensions in deep-time S2S studies.

7.2 | Scaling relationships of rift S2S segments with transverse and axial routing systems

Morphological relationships have been widely proven to exist between S2S routing segments in modern systems. A good example is the positive relationship between the submarine fan area and drainage basin area (e.g., Nyberg et al., 2018; Romans, Castelltort, Covault, Fildani, & Walsh, 2016; Sømme et al., 2009; Sømme & Jackson, 2013; Sømme, Jackson, et al., 2013). Although these scaling relationships come from a range of settings, and from systems that range in scale from very large (e.g., Niger) to very small (e.g., Golo) (e.g., Nyberg et al., 2018; Sømme et al., 2009), there is still controversy about whether such relationships hold true for different tectonic settings, or for older, deep-time S2S systems (e.g., Helland-Hansen et al., 2016; Nyberg et al., 2018).

Sømme et al. (2009) showed tectonically active basins to exhibit the poorest correlation between drainage basin area and basin floor fan area, a phenomenon that the authors attributed to the tendency for small fans along tectonically active margins to be fed by several small drainage basins rather than a single large drainage basin. However, in this study, we have found that the slope of the basin floor topography in the Kendrew Trough has a strong influence on the length-to-thickness ratio of fan deposits, irrespective of drainage basin size. The submarine fan immediately above the J53.0 horizon in the D5 depocenter develops a length of *ca*. 1.8 km and a thickness of *ca*. 320 m (Figure 11a,c). However, when topography in the Kendrew Trough flattens out near the D4 depocenter, the submarine fan on this same stratigraphic horizon extends further basinward, over a distance of *ca*. 7.5 km, and shows a decreased thickness to *ca*. 210 m (Figure 11a,d). Thus, if one is to examine the scaling relationships of these different elements of the S2S systems, in addition to influences such as drainage basin areas, the influence of the depositional surface slope and accommodation must be taken into account.

In many tectonically active settings, sediment dispersal from basin margin sediment sources to basin floor sediment sinks is not only characterized by small transverse fans that can be related to specific drainage basins, but sediment transport is also highly three dimensional with significant axial (i.e., parallel to strike) sediment transport. Such axial deep-water routing systems are well documented in deep-water foreland fold and thrust belts (e.g., Alpine and Pyrenean foreland basins; Bentham, Burbank, & Puigdefabregas, 1992; Hülscher, Fischer, Grunert, Auer, & Bernhardt, 2019; Sharman et al., 2018) and in salt-influenced passive margins (e.g., Oluboyo, Gawthorpe, Bakke, & Hadler-Jacobsen, 2014). A key characteristic of the deep-water depositional systems in the Kendrew Trough is the presence of an axial turbite fairway outboard of, and interfingering with, footwall-sourced, transverse submarine fan complexes (Figures 11 and 12). The interfingering of the transverse and axial segments of the sediment routing system in the basin poses difficulty in correctly assigning individual fan complexes to their up-dip feeding drainage domains (Figure 13). Furthermore, axial systems transport sediment many tens of kilometres along strike from their feeder catchments to their depositional sinks (Figure 13). The channel dominated axial system in the Kendrew Trough also seems to trim the toes of some transverse submarine fans and hence transfers this sediment along strike, further down the axial routing segment (Figure 12). These processes result in net sediment loss in some areas closer to the source of the axial flowing turbidites, and net gain farther down the transport pathway where these sediments are re-deposited (Figures 11, 12a–c, and 13). In the Kendrew Trough, nearly all submarine fan complex areas are smaller than predicted by the general catchment area-fan area relationship derived by Nyberg et al. (2018), indicating the major re-depositional area may be out of the study area, more south-westward in the Kendrew Trough (Figure 7d). Furthermore, no simple positive or negative bias tendency of catchment-fan area ratios compared with that of Nyberg et al. (2018) exists along the flow direction of axial turbidite between these submarine fan complexes, which implicates more controls, such as the geometry of Rankin Fault System and topography of the Kendrew Trough, influence these sediment redistributive processes. These observations suggest that, although the databases of Sømme et al. (2009) and Nyberg et al. (2018) are extensive, they might not be the best references for small-scale rift basins in late syn-rift and post-rift stages during which complex sediment redistributive processes occur due to the interaction of transverse and

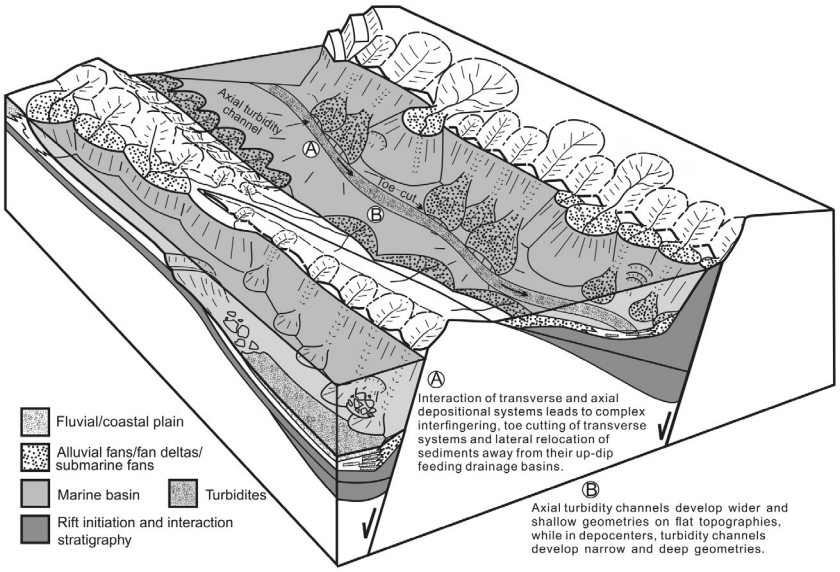

FIGURE 13 Conceptual architectural model of the interactions between transverse submarine fan systems and axial turbidity channels in the late syn-rift and post-rift stage of marine rift basins. The base map is modified from Gawthorpe and Leeder (2000)

axial depositional systems (e.g., Gawthorpe & Leeder, 2000), a similar process that has been noted in continental rift basin (e.g., Leeder & Mack, 2001).

7.3 | Syn-rift deep-water depositional systems

Deep-water depositional systems are common elements of the syn-rift stratigraphy of rift basins, typically within rift climax times when fault-controlled subsidence outpaces sediment supply leading to the development of deep-water, sediment starvation conditions (e.g., Cowie, Gupta, & Dawers, 2008; Gawthorpe & Leeder, 2000; Leeder & Gawthorpe, 1987; Prosser, 1993; Ravnås & Steel, 1998). Transverse syn-rift deep-water depositional systems are commonly depicted as lobate deposits at the base of steep faulted scarps, sourced from small catchments developed along rift-margin border faults or down-dip of major deltaic systems sourced from major rift hinterland drainages (e.g., East Greenland; Henstra et al., 2016; Surlyk, 1989); North Sea (Stow, Bishop, & Mills, 1982; Turner, Bastidas, Connell, & Petrik, 2018); Corinth (Ford, Hemelsdaël, Mancini, & Palyvos, 2017; Gawthorpe et al., 2018; Rohais, Eschard, Ford, Guillocheau, & Moretti, 2007) and Gulf of Suez (Leppard & Gawthorpe, 2006; Sharp, Gawthorpe, Underhill, & Gupta, 2000; Strachan et al., 2013). Transverse deep-water systems are also recognized in the immediate hanging wall of fault-controlled slopes associated with small catchments developed on intra-rift footwall highs, or from the degradation of the crest and scarp of these highs (e.g., North Sea; McArthur, Hartley, Archer, Jolley, & Lawrence, 2016; Underhill, Sawyer, Hodgson, Shallcross, & Gawthorpe, 1997); Corinth (Papatheodorou & Ferentinos, 1993). In comparison, axial deep-water syn-rift systems are commonly documented as longer run-out, deep-water channel-lobe complexes, elongate along hanging wall depocenters predominantly within rift axis of fault blocks (e.g., North Sea; Fraser et al., 2003; McArthur et al., 2016); Gulf of Corinth (Gawthorpe et al., 2018; McNeill et al., 2005; Muravchik et al., 2019). These axial depositional systems may be located many tens of kilometres along strike from the basin margin transverse systems that feed them (e.g., Gawthorpe et al., 2018).

Mixed syn-rift deep-water systems, where transverse and axial depositional systems interplay and interfinger within the same fault block depocenter, are comparatively less well documented. Examples include East African Rift System (e.g., Soreghan, Scholz, & Wells, 1999; Zhang & Scholz, 2015); Corinth Rift (Cullen, Collier, Gawthorpe, Hodgson, & Barrett, 2019; Gawthorpe et al., 2018); North Sea (McArthur et al., 2016). The seismic geomorphology and well penetrations in the hanging wall of the Rankin Fault System provide important new insights into the interaction of deep-water transverse and axial depositional systems in rift basins sourced from major intra-rift highs (Rankin Platform). Compared to many other transverse deep-water fan complexes deposited in the Kendrew Trough are relatively large, extending up to *ca*. 9 km into the immediate hanging wall of the Rankin Fault System (Figure 11). Core data suggest deposition from sediment gravity flows similar to those interpreted to be responsible for the deposition of Late Jurassic to Early Cretaceous syn-rift submarine fans in the hanging wall of the Dombjerg Fault in East Greenland (e.g., Henstra et al., 2016).

The toes of these transverse fans show complex stratigraphic relationships with the contemporaneous axial turbidite channel complex that developed along the axis of the Kendrew Trough. In deep marine syn-rift systems interaction of transverse and axial depositional systems is relatively poorly documented. Most studies suggest that the axial system "reacts" to sea-floor topography associated with the

transverse depositional systems. For example, in the Gulf of Corinth, Cullen et al. (2019) demonstrated the deflection of an axial turbidite system of up to 3 km away from the active fault scarp due to the topography of transverse mass transport deposits derived from the footwall scarp. Although a similar relationship may exist in the Kendrew Trough, the most striking aspect of the stratigraphic relationships between the transverse and axial depositional systems is the apparent erosion of the oldest unit of transverse fan complexes by the axial turbiditic channel system (Figures 11–13). Such relationships are reminiscent of the relationships of axial rivers and toe-trimmed alluvial fans from terrestrial rift basins (e.g., Leeder & Mack, 2001). The significance of erosion and toe cutting by axial turbiditic channel systems has not been recognized in deep-water depositional systems and can lead to sharp facies juxtaposition of relatively poorly sorted debris flows of the transverse fans and relatively better sorted axial turbidite sands. The mechanisms promoting deflection of axial systems by transverse fans versus toe cutting of transverse fans by axial turbidite systems requires further research, but plausible mechanisms include disequilibrium in the magnitude and frequency of gravity flows between the transverse fans and axial channels, or tilting of the hanging wall causing lateral migration or avulsion of the axial turbidite channels towards the fault.

8 | CONCLUSION

The nature of a depositional basin's drainage network and contributing drainage basins are important variables that influence the ultimate nature of basin filling (i.e., timing, duration, sedimentology and stratigraphy). Unfortunately, in palaeo-basins, the original drainage basins are often removed by subsequent erosion, or, not being the primary region of exploration interest, have little subsurface industry data documenting their nature. This lack of data over regions of the deep-time drainage systems limits the analogue utilization of morphological scaling relationships derived in modern systems. This study in the Dampier Sub-basin of the Northwest Shelf of Australia offers a well-documented (seismic, logs and core) example of an ancient rift basin where both the drainages and the downdip submarine deposits can be examined and relationships derived between basin elements. These results are compared with modern analogue studies to examine the strength and weaknesses of such derived relationships and to assess those variables that are most influential in rift basin source-to-sink sediment partition. Key conclusions include:

1. The hydrological and geomorphologic analysis identifies 24 preserved drainage basins on the J50.0 (Tithonian) erosional surface of the Rankin Platform, which is further grouped into six drainage domains, with areas ranging between 29 and 156 km^2. Drainage outlets of these drainage domains are clearly imaged on seismic data, with cross-sectional areas ranging from 0.08 to 0.31 km^2. The sedimentological and geomorphological analysis shows transverse submarine fan complexes developed in the Kendrew Trough, toe trimmed by rift-axial turbidity channels, resulting in final areas ranging from 43 to 193 km^2.
2. Geomorphological analysis of footwall catchments shows positive scaling relationships between the drainage domain areas and the cross-sectional area of drainage outlets and between drainage basin lengths and drainage outlet spacings. Thus, using a combination of drainage outlet spacing and cross-sectional area can provide important constraints on source area dimensions in deep-time S2S studies, especially in studies without preservation of the up-dip drainage basins.
3. Scaling relationships of rift S2S segments suggest a broadly negative bias of submarine fan complex areas to drainage domain area ratios, which implicate net sediment losses in submarine fan complexes by axial turbidite system erosion as the cause. The influence of tectonic topography on the three-dimensional distribution of depositional system morphology should also be taken into account.
4. Transverse submarine fans may show deflection down rift and/or be toe trimmed. Erosion and toe cutting of transverse submarine fans by axial turbiditic channel systems can lead to sharp facies juxtaposition of relatively poorly sorted debris flows of the transverse fans and relatively better sorted axial turbidite sands. Plausible mechanisms causing interactions of transverse fans and axial turbidite systems include disequilibrium in the magnitude and frequency of gravity flows between the transverse fans and axial channels, or tilting of the hanging wall causing lateral migration or avulsion of the axial turbidite channels towards the fault.

ACKNOWLEDGEMENTS

We would like to thank the consortium members of the Colorado School of Mines Sedimentary Analogs Database and Research program (SAnD) for their support on this work. Woodside Energy Ltd. and its partners are especially acknowledged for providing optimized seismic reflection data, and the authors would like to thank Eujay McCartain and other geoscientists in Woodside for their active collaboration on the science in this work. Geoscience Australia is thanked for providing access to well data. We would like to thank reviewers Dr. Christopher Jackson, Dr. Johan Claringbould and Dr. Brian Jones for their contributed comments which significantly improved this manuscript. This work was partly undertaken at the University of Bergen when Dr. Chen was

funded as a VISTA visiting researcher under the VISTA professorship awarded to Dr. Gawthorpe.

ORCID

Hehe Chen https://orcid.org/0000-0003-0312-0764
Robert L. Gawthorpe https://orcid.org/0000-0002-4352-6366

REFERENCES

Anderson, J. B., Wallace, D. J., Simms, A. R., Rodriguez, A. B., & Taha, Z. P. (2016). Recycling sediments between source and sink during a eustatic cycle: Systems of the late quaternary northwestern Gulf of Mexico Basin. *Earth-Science Reviews*, *153*, 111–138.

Barber, P. (1994). Late jurassic-early cretaceous depositional systems of the dampier sub-basin-quo vadis?. *The APPEA Journal*, *34*(1), 566–585. https://doi.org/10.1071/AJ93044

Bentham, P. A., Burbank, D. W., & Puigdefabregas, C. A. I. (1992). Temporal and spatial controls on the alluvial architecture of an axial drainage system: Late Eocene Escanilla Formation, southern Pyrenean foreland basin, Spain. *Basin Research*, *4*(3–4), 335–352. https://doi.org/10.1111/j.1365-2117.1992.tb00052.x

Bhattacharya, J. P., Copeland, P., Lawton, T. F., & Holbrook, J. (2016). Estimation of source area, river paleo-discharge, paleoslope, and sediment budgets of linked deep-time depositional systems and implications for hydrocarbon potential. *Earth-Science Reviews*, *153*, 77–110. https://doi.org/10.1016/j.earscirev.2015.10.013

Blum, M., Martin, J., Milliken, K., & Garvin, M. (2013). Paleovalley systems: Insights from Quaternary analogs and experiments. *Earth-Science Reviews*, *116*, 128–169. https://doi.org/10.1016/j.earscirev.2012.09.003

Cathro, D. L., & Karner, G. D. (2006). Cretaceous-Tertiary inversion history of the Dampier Sub-basin, northwest Australia: Insights from quantitative basin modelling. *Marine and Petroleum Geology*, *23*(4), 503–526. https://doi.org/10.1016/j.marpetgeo.2006.02.005

Chen, H. H., Zhu, X. M., Wood, L., & Shi, R. S. (2019). Evolution of drainage, sediment-flux and fluvio-deltaic sedimentary systems response in hanging wall depocentres in evolving non-marine rift basins: Paleogene of Raoyang Sag, Bohai Bay Basin. *China. Basin Research*, *32*(1), 116–145. https://doi.org/10.1111/bre.12371

Connell, S. D., Kim, W., Paola, C., & Smith, G. A. (2012). Fluvial morphology and sediment-flux steering of axial-transverse boundaries in an experimental basin. *Journal of Sedimentary Research*, *82*(5), 310–325. https://doi.org/10.2110/jsr.2012.27

Cowie, P. A., Gupta, S., & Dawers, N. H. (2008). Implications of fault array evolution for synrift depocentre development: insights from a numerical fault growth model. *Basin Research*, *12*(3–4), 241–261.

Cullen, T. M., Collier, R. E. L., Gawthorpe, R. L., Hodgson, D. M., & Barrett, B. J. (2019). Axial and transverse deep-water sediment supply to syn-rift fault terraces: Insights from the West Xylokastro Fault Block, Gulf of Corinth, Greece. *Basin Research*, 1–35. https://doi.org/10.1111/bre.12416

Densmore, A. L., Dawers, N. H., Gupta, S., Allen, P. A., & Gilpin, R. (2003). Landscape evolution at extensional relay zones. *Journal of Geophysical Research: Solid Earth*, *108*(B5).1–15.

Densmore, A. L., Dawers, N. H., Gupta, S., & Guidon, R. (2005). What sets topographic relief in extensional footwalls? *Geology*, *33*(6), 453–456. https://doi.org/10.1130/G21440.1

DiBiase, R. A., Whipple, K. X., Heimsath, A. M., & Ouimet, W. B. (2010). Landscape form and millennial erosion rates in the San Gabriel Mountains, CA. *Earth and Planetary Science Letters*, *289*(1–2), 134–144. https://doi.org/10.1016/j.epsl.2009.10.036

Duffy, O. B., Brocklehurst, S. H., Gawthorpe, R. L., Leeder, M. R., & Finch, E. (2015). Controls on landscape and drainage evolution in regions of distributed normal faulting: Perachora Peninsula, Corinth Rift, Central Greece. *Basin Research*, *27*(4), 473–494. https://doi.org/10.1111/bre.12084

Elliott, G. M., Wilson, P., Jackson, C. A. L., Gawthorpe, R. L., Michelsen, L., & Sharp, I. R. (2012). The linkage between fault throw and footwall scarp erosion patterns: An example from the Bremstein Fault Complex, offshore Mid-Norway. *Basin Research*, *24*(2), 180–197. https://doi.org/10.1111/j.1365-2117.2011.00524.x

Ethridge, F. G., Germanoski, D., Schumm, S. A., & Wood, L. J. (2005). The morphological and stratigraphical effects of base-level change: A review of experimental studies. *Fluvial Sedimentology VII*, *35*, 213–241.

Ford, M., Hemelsdaël, R., Mancini, M., & Palyvos, N. (2017). Rift migration and lateral propagation: Evolution of normal faults and sediment-routing systems of the western Corinth rift (Greece). *Geological Society, London, Special Publications*, *439*(1), 131–168. https://doi.org/10.1144/SP439.15

Fraser, S., Robinson, A., Johnson, H., Underhill, J., Kadolsky, D., Connel, R., … Ravnås, R. (2003). Upper Jurassic. I. D. Evans, C. Graham, A. Armour, & P. Bathurst (Eds.), *The millennium atlas: Petroleum geology of the central and northern North Sea* (pp. 157–189). London: Geological Society of London.

Fullerton, L. G., Sager, W. W., & Handschumacher, D. W. (1989). Late Jurassic-early cretaceous evolution of the eastern Indian Ocean adjacent to northwest Australia. *Journal of Geophysical Research: Solid Earth*, *94*(B3), 2937–2953. https://doi.org/10.1029/JB094iB03p02937

Gawthorpe, R. L., & Leeder, M. R. (2000). Tectono-sedimentary evolution of active extensional basins. *Basin Research*, *12*, 195–218. https://doi.org/10.1046/j.1365-2117.2000.00121.x

Gawthorpe, R. L., Leeder, M. R., Kranis, H., Skourtsos, E., Andrews, J. E., Henstra, G. A., … Stamatakis, M. (2018). Tectono-sedimentary evolution of the Plio-Pleistocene Corinth rift, Greece. *Basin Research*, *30*(3), 448–479. https://doi.org/10.1111/bre.12260

Helland-Hansen, W., Sømme, T. O., Martinsen, O. J., Lunt, I., & Thurmond, J. (2016). Deciphering Earth's natural hourglasses: Perspectives on source-to-sink analysis. *Journal of Sedimentary Research*, *86*(9), 1008–1033. https://doi.org/10.2110/jsr.2016.56

Henstra, G. A., Grundvåg, S.-A., Johannessen, E. P., Kristensen, T. B., Midtkandal, I., Nystuen, J. P., … Windelstad, J. (2016). Depositional processes and stratigraphic architecture within a coarse-grained rift-margin turbidite system: The Wollaston Forland Group, east Greenland. *Marine and Petroleum Geology*, *76*, 187–209. https://doi.org/10.1016/j.marpetgeo.2016.05.018

Hill, G. (1994). The role of the pre-rift structure in the architecture of the Dampier Basin area, North West Shelf, Australia. *The APPEA Journal*, *34*(1), 602–613. https://doi.org/10.1071/AJ93046

Hovius, N. (1996). The regular spacing of drainage outlets from linear mountain belts. *Basin Research*, *8*(1), 29–44. https://doi.org/10.1111/j.1365-2117.1996.tb00113.x

Hülscher, J., Fischer, G., Grunert, P., Auer, G., & Bernhardt, A. (2019). Selective recording of tectonic forcings in an Oligocene/Miocene submarine channel system: Insights from new age constraints and

sediment volumes from the Austrian Northern Alpine Foreland Basin. *Frontiers in Earth Science*, *7*, 1–25.

Jablonski, D. (1997). Recent advances in the sequence stratigraphy of the Triassic to lower Cretaceous succession in the northern Carnarvon Basin, Australia. *The APPEA Journal*, *37*(1), 429–454. https://doi.org/10.1071/AJ96026

Leeder, M. R. (2011). Tectonic sedimentology: Sediment systems deciphering global to local tectonics. *Sedimentology*, *58*(1), 2–56. https://doi.org/10.1111/j.1365-3091.2010.01207.x

Leeder, M. R., & Gawthorpe, R. L. (1987). Sedimentary models for extensional tilt-block/half-graben basins. *Geological Society, London, Special Publications*, *28*(1), 139–152.

Leeder, M. R., & Jackson, J. A. (1993). The interaction between normal faulting and drainage in active extensional basins, with examples from the western United States and central Greece. *Basin Research*, *5*(2), 79–102. https://doi.org/10.1111/j.1365-2117.1993.tb00059.x

Leeder, M. R., & Mack, G. H. (2001). Lateral erosion ('toe-cutting') of alluvial fans by axial rivers: Implications for basin analysis and architecture. *Journal of the Geological Society*, *158*(6), 885–893. https://doi.org/10.1144/0016-760000-198

Leeder, M. R., Seger, M. J., & Stark, C. P. (1991). Sedimentation and tectonic geomorphology adjacent to major active and inactive normal faults, southern Greece. *Journal of the Geological Society*, *148*(2), 331–343. https://doi.org/10.1144/gsjgs.148.2.0331

Leppard, C. W., & Gawthorpe, R. L. (2006). Sedimentology of rift climax deep water systems; lower Rudeis formation, Hammam Faraun fault block, Suez Rift, Egypt. *Sedimentary Geology*, *191*(1–2), 67–87. https://doi.org/10.1016/j.sedgeo.2006.01.006

Liu, H., van Loon, A. J., Xu, J., Tian, L., Du, X., Zhang, X., & Chen, D. (2019). Relationships between tectonic activity and sedimentary source-to-sink system parameters in a lacustrine rift basin: A quantitative case study of the Huanghekou Depression (Bohai Bay Basin, E China). *Basin Research*, 1–26.

Longley, I. M., Buessenschuett, C., Clydsdale, L., Cubitt, C. J., Davis, R. C., Johnson, M. K., … Thompson, N. B. (2002). The north west shelf of Australia—A Woodside perspective. In M. Keep & S. J. Moss (Eds.), *The Sedimentary Basins of Western Australia 3: Proceedings of the Petroleum Exploration Society of Australia Symposium, Perth* (pp. 27–88). Perth, Australia: Petroleum Exploration Society of Australia.

Marshall, N. G., & Lang, S. C. (2013). A new sequence stratigraphic framework for the North West Shelf, Australia. In *The Sedimentary Basins of Western Australia 4: Proceedings PESA Symposium. Perth* (pp. 1–32).

Matenco, L., & Andriessen, P. (2013). Quantifying the mass transfer from mountain ranges to deposition in sedimentary basins: Source to sink studies in the Danube Basin-Black Sea system. *Global and Planetary Change*, *103*, 1–18. https://doi.org/10.1016/j.gloplacha.2013.01.003

Mattheus, C. R., & Rodriguez, A. B. (2011). Controls on late Quaternary incised-valley dimension along passive margins evaluated using empirical data. *Sedimentology*, *58*(5), 1113–1137. https://doi.org/10.1111/j.1365-3091.2010.01197.x

Mattheus, C. R., & Rodriguez, A. B. (2014). Controls on lower-coastal-plain valley morphology and fill architecture. *Journal of Sedimentary Research*, *84*(4), 314–325. https://doi.org/10.2110/jsr.2014.30

Mattheus, C. R., Rodriguez, A. B., Greene, D. L., Simms, A. R., & Anderson, J. B. (2007). Control of upstream variables on incised-valley dimension. *Journal of Sedimentary Research*, *77*(3), 213–224. https://doi.org/10.2110/jsr.2007.022

McArthur, A. D., Hartley, A. J., Archer, S. G., Jolley, D. W., & Lawrence, H. M. (2016). Spatiotemporal relationships of deep-marine, axial, and transverse depositional systems from the synrift Upper Jurassic of the central North Sea. *AAPG Bulletin*, *100*(9), 1469–1500. https://doi.org/10.1306/04041615125

McHarg, S., Elders, C., & Cunneen, J. (2019a). Normal fault linkage and reactivation, Dampier Sub-basin, Western Australia. *Australian Journal of Earth Sciences*, *66*(2), 209–225. https://doi.org/10.1080/08120099.2019.1519848

McHarg, S., Elders, C., & Cunneen, J. (2019b). Origin of basin-scale syn-extensional synclines on the southern margin of the Northern Carnarvon Basin, Western Australia. *Journal of the Geological Society*, *176*(1), 115–128. https://doi.org/10.1144/jgs2018-043

McNeill, L. C., Cotterill, C. J., Henstock, T. J., Bull, J. M., Stefatos, A., Collier, R. E. L., … Hicks, S. E. (2005). Active faulting within the offshore western Gulf of Corinth, Greece: Implications for models of continental rift deformation. *Geology*, *33*(4), 241–244. https://doi.org/10.1130/G21127.1

Milliman, J. D., & Syvitski, J. P. (1992). Geomorphic/tectonic control of sediment discharge to the ocean: The importance of small mountainous rivers. *The Journal of Geology*, *100*(5), 525–544. https://doi.org/10.1086/629606

Muravchik, M., Henstra, G. A., Eliassen, G. T., Gawthorpe, R. L., Leeder, M., Kranis, H., … Andrews, J. (2019). Deep-water sediment transport patterns and basin floor topography in early rift basins: Plio-Pleistocene syn-rift of the Corinth Rift, Greece. *Basin Research*, 1–29. https://doi.org/10.1111/bre.12423

Nyberg, B., Helland-Hansen, W., Gawthorpe, R. L., Sandbakken, P., Eide, C. H., Sømme, T., … Leiknes, S. (2018). Revisiting morphological relationships of modern source-to-sink segments as a first-order approach to scale ancient sedimentary systems. *Sedimentary Geology*, *373*, 111–133. https://doi.org/10.1016/j.sedgeo.2018.06.007

Oluboyo, A. P., Gawthorpe, R. L., Bakke, K., & Hadler-Jacobsen, F. (2014). Salt tectonic controls on deep-water turbidite depositional systems: Miocene, southwestern Lower Congo Basin, offshore Angola. *Basin Research*, *26*(4), 597–620. https://doi.org/10.1111/bre.12051

Papatheodorou, G., & Ferentinos, G. (1993). Sedimentation processes and basin-filling depositional architecture in an active asymmetric graben: Strava graben, Gulf of Corinth. *Greece. Basin Research*, *5*(4), 235–253. https://doi.org/10.1111/j.1365-2117.1993.tb00069.x

Pechlivanidou, S., Cowie, P. A., Duclaux, G., Nixon, C. W., Gawthorpe, R. L., & Salles, T. (2019). Tipping the balance: Shifts in sediment production in an active rift setting. *Geology*, *47*(3), 259–262. https://doi.org/10.1130/G45589.1

Prosser, S. (1993). Rift-related linked depositional systems and their seismic expression. *Geological Society, London, Special Publications*, *71*(1), 35–66.

Ravnås, R., & Steel, R. J. (1998). Architecture of marine rift-basin successions. *AAPG bulletin*, *82*(1), 110–146.

Rohais, S., Eschard, R., Ford, M., Guillocheau, F., & Moretti, I. (2007). Stratigraphic architecture of the Plio-Pleistocene infill of the Corinth Rift: Implications for its structural evolution. *Tectonophysics*, *440*(1–4), 5–28. https://doi.org/10.1016/j.tecto.2006.11.006

Romans, B. W., Castelltort, S., Covault, J. A., Fildani, A., & Walsh, J. P. (2016). Environmental signal propagation in sedimentary systems across timescales. *Earth-Science Reviews*, *153*, 7–29. https://doi.org/10.1016/j.earscirev.2015.07.012

Sharman, G. R., Hubbard, S. M., Covault, J. A., Hinsch, R., Linzer, H. G., & Graham, S. A. (2018). Sediment routing evolution in the North Alpine Foreland Basin, Austria: Interplay of transverse and longitudinal sediment dispersal. *Basin Research*, *30*(3), 426–447. https://doi.org/10.1111/bre.12259

Sharp, I. R., Gawthorpe, R. L., Underhill, J. R., & Gupta, S. (2000). Fault-propagation folding in extensional settings: Examples of structural style and synrift sedimentary response from the Suez rift, Sinai. *Egypt. Geological Society of America Bulletin*, *112*(12), 1877–1899. https://doi.org/10.1130/0016-7606(2000)112<1877:FPFIES>2.0.CO;2

Sømme, T. O., Helland-Hansen, W., Martinsen, O. J., & Thurmond, J. B. (2009). Relationships between morphological and sedimentological parameters in source-to-sink systems: A basis for predicting semi-quantitative characteristics in subsurface systems. *Basin Research*, *21*(4), 361–387. https://doi.org/10.1111/j.1365-2117.2009.00397.x

Sømme, T. O., & Jackson, C. A. L. (2013). Source-to-sink analysis of ancient sedimentary systems using a subsurface case study from the Møre-Trøndelag area of southern Norway: Part 2-sediment dispersal and forcing mechanisms. *Basin Research*, *25*(5), 512–531. https://doi.org/10.1111/bre.12014

Sømme, T. O., Jackson, C. A. L., & Vaksdal, M. (2013). Source-to-sink analysis of ancient sedimentary systems using a subsurface case study from the Møre-Trøndelag area of southern Norway: Part 1-depositional setting and fan evolution. *Basin Research*, *25*(5), 489–511. https://doi.org/10.1111/bre.12013

Soreghan, M. J., Scholz, C. A., & Wells, J. T. (1999). Coarse-grained, deep-water sedimentation along a border fault margin of Lake Malawi, Africa; seismic stratigraphic analysis. *Journal of Sedimentary Research*, *69*(4), 832–846. https://doi.org/10.2110/jsr.69.832

Stagg, H. M. J. (2004). *Geological framework of the outer Exmouth Plateau and adjacent ocean basins*, Canberra : Geoscience Australia.

Stow, D. A., Bishop, C. D., & Mills, S. J. (1982). Sedimentology of the Brae oilfield, North Sea: Fan models and controls. *Journal of Petroleum Geology*, *5*(2), 129–148. https://doi.org/10.1111/j.1747-5457.1982.tb00501.x

Strachan, L. J., Rarity, F., Gawthorpe, R. L., Wilson, P., Sharp, I., & Hodgetts, D. (2013). Submarine slope processes in rift-margin basins, Miocene Suez Rift, Egypt. *Geological Society of America Bulletin*, *125*(1–2), 109–127. https://doi.org/10.1130/B30665.1

Surlyk, F. (1989). Mid-Mesozoic syn-rift turbidite systems: Controls and predictions. In J. Collinson (Ed.), *Correlation in hydrocarbon exploration* (pp. 231–241). Dordrecht, the Netherlands: Springer.

Talling, P. J., Stewart, M. D., Stark, C. P., Gupta, S., & Vincent, S. J. (1997). Regular spacing of drainage outlets from linear fault blocks. *Basin Research*, *9*(4), 275–302. https://doi.org/10.1046/j.1365-2117.1997.00048.x

Thomas, G. P., Lennane, M. R., Glass, F., Walker, T., Partington, M., Leischner, K. R., & Davis, R. C. (2004). Breathing new life into the eastern Dampier Sub-basin: An integrated review based on geophysical, stratigraphic and basin modelling evaluation. *The APPEA Journal*, *44*(1), 123–150. https://doi.org/10.1071/AJ03004

Turner, C. C., Bastidas, R. E., Connell, E. R., & Petrik, F. E. (2018). Proximal submarine fan reservoir architecture and development in the Upper Jurassic Brae Formation of the Brae fields, South Viking Graben, UK North Sea. In C. C. Turner & B. T. Cronin (Eds.), *Rift-related coarse-grained submarine fan reservoirs; The Brae Play, South Viking Graben, North Sea: AAPG Memoir 115* (pp. 213–256). Tulsa, OK: AAPG.

Underhill, J. R., Sawyer, M. J., Hodgson, P., Shallcross, M. D., & Gawthorpe, R. L. (1997). Implications of fault scarp degradation for Brent group prospectivity, Ninian field, northern North Sea. *AAPG Bulletin*, *81*(6), 999–1022.

Walcott, R. C., & Summerfield, M. A. (2009). Universality and variability in basin outlet spacing: Implications for the two-dimensional form of drainage basins. *Basin Research*, *21*(2), 147–155. https://doi.org/10.1111/j.1365-2117.2008.00379.x

Watkins, S. E., Whittaker, A. C., Bell, R. E., McNeill, L. C., Gawthorpe, R. L., Brooke, S. A., & Nixon, C. W. (2018). Are landscapes buffered to high-frequency climate change? A comparison of sediment fluxes and depositional volumes in the Corinth Rift, central Greece, over the past 130 ky. *GSA Bulletin*, *131*(3–4), 372–388.

Whittaker, A. C., Attal, M., & Allen, P. A. (2010). Characterising the origin, nature and fate of sediment exported from catchments perturbed by active tectonics. *Basin Research*, *22*(6), 809–828.

Wood, L. J. (2007). Quantitative seismic geomorphology of Pliocene and Miocene fluvial systems in the northern Gulf of Mexico, USA. *Journal of Sedimentary Research*, *77*(9), 713–730. https://doi.org/10.2110/jsr.2007.068

Woodside. (2007). Dixon-2, Well Completion Report, Basic Data, WA-9-R, Dampier Sub-basin. P376.

Wu, D., Zhu, X., Su, Y., Li, Y., Li, Z., Zhou, Y., & Zhang, M. (2015). Tectono-sequence stratigraphic analysis of the lower cretaceous Abu Gabra formation in the Fula sub-basin, Muglad basin, southern Sudan. *Marine and Petroleum Geology*, *67*, 286–306. https://doi.org/10.1016/j.marpetgeo.2015.05.024

Zhang, X., & Scholz, C. A. (2015). Turbidite systems of lacustrine rift basins: Examples from the Lake Kivu and Lake Albert rifts, East Africa. *Sedimentary Geology*, *325*, 177–191. https://doi.org/10.1016/j.sedgeo.2015.06.003

How to cite this article: Chen H, Wood LJ, Gawthorpe RL. Sediment dispersal and redistributive processes in axial and transverse deep-time source-to-sink systems of marine rift basins: Dampier Sub-basin, Northwest Shelf, Australia. *Basin Res*. 2020;00:1–23. https://doi.org/10.1111/bre.12462